

TELEMAC IST 2000-28156

Telemonitoring and Advanced Telecontrol of High-Yield Wastewater Treatment

Development of set of robust controllers with various objectives

FINAL VERSION of Deliverable D3.3

*Deliverable type: Report**Number: D3.3**Nature: model design**Delivery of first version: 15th January 2004**Delivery of final version: 8th June 2004**Task WP3.3**Responsible:**Frédéric Grognard**Inria-Sophia BP 93**06902 Sophia-Antipolis Cedex**Email: olivier.bernard@inria.fr**Other contributors:*

<i>O. Bernard, A. Hélias and L.Mailleret</i>	<i>INRIA</i>
<i>J. Rodriguez and G. Ruiz</i>	<i>USC</i>
<i>J.-P. Steyer and L. Lardon</i>	<i>INRA</i>
<i>P.Ratini</i>	<i>SPES</i>
<i>J.F-Lavigne</i>	<i>Allied Domecq</i>
<i>C. A. Aceves-Lara, V. Alcaraz-González, O. González-Reynoso, E. Aguilar- Garnica, and V. González-Álvarez.</i>	<i>UdG</i>
<i>P. Lemaire</i>	<i>P.L.</i>

Reviewers:

<i>J.-P. Steyer</i>	<i>INRA</i>
<i>V. Alcaraz-González.</i>	<i>UdG</i>
<i>J. Rodriguez</i>	<i>USC</i>

Abstract: This report presents the various controllers that have been developed for TELEMAC. The different teams have tackled several control objectives: the control of the COD, which represents the pollution level in the plant; the control of the VFA, to avoid acidification of the plant; and the control of the cogeneration ratio, which represents the quality of the methane production. Using the methane flow-rate, the VFA concentration, or the COD measurements, control methods ranging from Lyapunov methods to fuzzy control have been used, and some have been experimentally validated.

Contents

Factual summary WP3.3	3
1 Model of anaerobic digestion	5
2 Control of the COD	6
2.1 Saturated control	6
2.1.1 Objective and constraints	6
2.1.2 Boundedness of the states	8
2.1.3 Control design	11
2.1.4 Interval observation	17
2.1.5 Simulations	18
2.1.6 Conclusion	20
2.2 Static output feedback using methane flow rate measurements	21
2.2.1 Study of a simplified model of the anaerobic digestion	22
2.2.2 Study of the dimension 4 model	24
2.2.3 Simulation study	27
2.2.4 Experimental results	29
2.2.5 Conclusion	30
2.3 Adaptive output feedback using methane flow rate measurements	31
2.3.1 Study of a simplified model of the anaerobic digestion	32
2.3.2 The problem of discrete time y_2 measurements	35
2.3.3 Simulations	35
2.3.4 Virtual plant	37
2.3.5 Conclusion	37
2.4 Simultaneous regulation of the substrate and the VFA	38
2.4.1 The regulation of S_1	38
2.4.2 The regulation of S_1 and S_2	41
2.4.3 Conclusion	42
2.5 Conclusion	42
3 Control of the VFA concentration	43
3.1 Material and methods	43
3.1.1 Anaerobic wastewater treatment plant	43
3.1.2 Control Law	44
3.2 Results and discussion	45
3.3 Conclusion	50
4 Control of the cogeneration ratio	51
4.1 The model	51
4.2 Dependence of the equilibrium value with respect to D	52
4.3 Dependence of the equilibrium value with respect to P_T	54
4.4 Dependence of the equilibrium value with respect to $k_L a$	54

4.5 Conclusion	56
5 Conclusion	57

Factual summary WP3.3

	Man-Months							
	INRIA	USC	INRA	SPES	Dcq	P.L.	UdG	
Recalls and state of the art								
– Anaerobic digestion modelling	0	0	0	0	0	0	0	
Developed controllers								
– Design of the Saturated Controller	0.8							
– Stability analysis of the Saturated Controller	1.3							
– Design of the static output feedback	0.4							
– Stability analysis of the static output feedback	2.5							
– Design of the adaptive output feedback	1.2							
– Stability analysis of the adaptive output feedback	3.7							
– Design of the simultaneous controller of S_1 and S_2	0.9						0.4	
– Stability analysis of the simultaneous controller	2.4						1.2	
– Design of the fuzzy controller			3.2	1.3				
– Tuning of the fuzzy controller			0.3	2.1				
– Static analysis of the cogeneration ratio	0.3							
– Industrial constraints and expert consulting	0	0	0	0	0.4	0.4		
Developed softwares								
– Matlab : simulations of the various controllers on small-scale models	0.7		0.2	0.3				
– Matlab : simulation of the controllers using measurements of the methane flow-rate on the virtual plant	2	1.2						
Validation and tests								
– Simulation and experimental testing of the static output feedback			0.5			0.2		
– Simulation and experimental testing of the fuzzy controller			0.3					
– Write deliverable D3.3	0.4							
Sum	16.6	1.2	4.5	3.7	0.4	0.6	1.6	
Total								28.6
Total EC partners								27

The control of bioreactors is a delicate problem since most of the time the available biological models are only rough approximations. Indeed, on the contrary to other domains (physics...) that use laws that have been tested and validated for centuries, the biological systems are known to be highly variable, difficult to measure so that no strong biological law is available. To circumvent this difficulty, Bastin and Dochain [1] have introduced the mass balance based modelling. The main idea of this approach is to design estimators and controllers independently of any modelling of the biological kinetics.

Among the bioreactors, those dedicated to wastewater treatment especially suffer from the modelling uncertainties. A complex ecosystem composed by many different bacterial populations takes place in these processes, and the composition and concentration of the pollutant to degrade is not well known and evolves with respect to time. Moreover, most of the time no measurement of the involved chemical or biological species is available. In these conditions, a control procedure that would guarantee the process stability should be as insensitive as possible to all these parameters.

We will consider an anaerobic wastewater treatment process. Anaerobic digestion is a biological process in which biodegradable organic materials are decomposed in the absence of oxygen to produce methane. The underlying model assumes that two main bacterial populations are present [3]. The first one, the acidogenic bacteria X_1 , consumes the organic substrate S_1 and produces through an acidogenesis step volatile fatty acids (VFA) S_2 . The second population (methanogenic bacteria) X_2 , uses the VFA in a methanogenesis step as substrate for growth and produces methane.

Despite its capacity to degrade difficult substrates, this process is known to become unstable under certain circumstances, like variations of the process operating conditions, and requires therefore a monitoring procedure to detect a destabilization. This must also be associated to a control action that can avoid the risk of acidification of the fermenter.

The considered model is the AM1 model that is presented in the Deliverable D3.1a. Several teams of the TELEMAT project have been working on the design of controllers, each trying to tackle a different control problem that was described in the definition of the project. The controllers that have been produced can be divided according to two criteria: the control objective and the measured variables. The three main objectives that have been pursued are:

- the control of the COD (Chemical Oxygen Demand). This variable is the standard measurement of the pollution level. In fact, the proposed controllers do not regulate the COD, but a biological equivalent of the total amount of organic substrate in the digester, that we will denote S_T or S_λ , depending on the formula that is used.
- the control of the Volatile Fatty Acids (VFA). It is generally shown that the limiting step in the biochemical degradation is the conversion of these VFA into methane. Therefore, if this reaction does not take place in appropriate conditions, and no attention is made to the concentration of VFA, those acids can accumulate and dangerously decrease the pH of the reactor. It is therefore wise to try and keep this variable under a certain threshold.
- the control of the cogeneration ratio, which is the ratio between the methane and carbon dioxide flow rates ($\frac{q_{CH_4}}{q_{CO_2}}$). The outgoing gaseous flow can be burned in an engine to provide energy to the plant. However, classical engines do not tolerate highly variable gaseous composition at their input. An efficient energy production therefore requires the regulation of cogeneration ratio.

The other differentiating aspect lies in the measured variables that are used in the control design

- the first class of controllers only use the outgoing methane flow rate, which is an “easily” measured quantity for the bioreactor.
- the second class of controllers use the Volatile Fatty Acid concentration measurement. In that purpose, a relatively inexpensive sensor, capable of measuring VFA, as well as partial and total alkalinity, based on a titrimetric method has been developed at INRA.
- the third class requires the knowledge of the measure of S_T or S_λ , which is equivalent to the knowledge of the COD.

In all cases, the variable that is used to control the bioreactor is the dilution rate (D). The control methods are very diverse: and they range from Lyapunov based design to fuzzy logic based control.

This report will be divided according to the control objective. The model is first recalled in Section 1. In Section 2, we present controllers that regulate the COD; we then give the controllers that tackle the VFA concentration regulation problem in Section 3. Finally, an insight on what could be done to regulate the cogeneration ratio is given in Section 4.

1 Model of anaerobic digestion

In this deliverable, we will solely use the model AM1 of anaerobic digestion.

$$\begin{cases} \dot{X}_1 &= (\mu_1(S_1) - \alpha D)X_1 \\ \dot{X}_2 &= (\mu_2(S_2) - \alpha D)X_2 \\ \dot{S}_1 &= D(S_{1in} - S_1) - k_1\mu_1(S_1)X_1 \\ \dot{S}_2 &= D(S_{2in} - S_2) + k_2\mu_1(S_1)X_1 - k_3\mu_2(S_2)X_2 \end{cases} \quad (1)$$

with $X_1, X_2, S_1, S_2, D \in \mathbb{R}^+$, $\mu_1(S_1) = \mu_{1max} \frac{S_1}{S_1 + K_{S_1}}$ a specific growth rate of the Monod type and $\mu_2(S_2) = \mu_{2max} \frac{S_2}{S_2 + K_{S_2} + \frac{S_2^2}{K_{I_2}}}$ a specific growth rate of the Haldane type. The Haldane function

reaches its maximum in $S_2 = \sqrt{K_{S_2} K_{I_2}}$, where it takes the value $\mu_{2max} \frac{\sqrt{K_{I_2}}}{\sqrt{K_{I_2} + 2} \sqrt{K_{S_2}}}$. The terms S_{1in} and S_{2in} are the influent concentrations of S_1 and S_2 respectively. The k_i represent the yield coefficients associated with bacterial growth. The parameter $\alpha \in [0, 1]$ represents the proportion of bacteria that are not fixed on the bed, and therefore which are affected by the dilution effect: $\alpha = 0$ would correspond to an ideal fixed bed reactor, $\alpha = 1$ to an ideal continuous stirred tank reactor. The stability analyses of the controlled bioreactors that we perform are mostly based on that model.

2 Control of the COD

2.1 Saturated control

2.1.1 Objective and constraints

The original control objective for depollution is to regulate the output $S_\lambda = S_1 + \lambda S_2$ (with $\lambda \geq 0$), at a value $\bar{S}_\lambda \leq S_{\lambda max} \leq S_{\lambda in} = S_{1in} + \lambda S_{2in}$. In this section, the objective is modified as follows

Objective 1 *Given $S_{\lambda min} \leq \bar{S}_\lambda \leq S_{\lambda max}$, steer all the solutions of the controlled system to a region where $S_{\lambda min} \leq S_\lambda \leq S_{\lambda max}$ is satisfied and stays valid for all future times*

Instead of achieving regulation, we will achieve attractivity and invariance of a security zone. In this formulation, $S_{\lambda max}$ is an unalterable data of the problem (fixed by depollution norms); on the other hand, $S_{\lambda min}$ can be chosen more freely: if it is taken close to $S_{\lambda max}$, the achievement of Objective 1 is almost equivalent to the regulation of the output S_λ ; if $S_{\lambda min}$ is taken close to zero, there is a risk that the system settles at a small value of S_λ with a small value of the dilution rate. The pollutant concentrations in the input, S_{1in} and S_{2in} , are supposed to be constant. They do not need to be known for the application of the controller. However, in order to show stability of the controller, those values need to be known.

In order to design a controller, we first analyze the different parameters of the problem, imposing conditions that they need to satisfy for the design of our controller.

The parameter λ The evolution of the pollution level follows the following equation:

$$\dot{S}_\lambda = D(S_{\lambda in} - S_\lambda) - (k_1 - \lambda k_2)\mu_1(S_1)X_1 - \lambda k_3\mu_2(S_2)X_2 \quad (2)$$

We will consider that $k_1 - \lambda k_2 > 0$; this condition is met by the identified parameters of the experimental process ([4]), and it has the advantage that the pollution level decreases when the flow rate is stopped. This condition is reasonable, as the main purpose of the plant is to eliminate S_1 .

The bound $S_{\lambda max}$ In the rest of this section, we will replace S_2 with the coordinate $T_2 = S_2 + \frac{k_2}{k_1}S_1$. This results in the following system:

$$\begin{cases} \dot{X}_1 &= (\mu_1(S_1) - \alpha D)X_1 \\ \dot{X}_2 &= (\mu_2(T_2 - \frac{k_2}{k_1}S_1) - \alpha D)X_2 \\ \dot{S}_1 &= D(S_{1in} - S_1) - k_1\mu_1(S_1)X_1 \\ \dot{T}_2 &= D(T_{2in} - T_2) - k_3\mu_2(T_2 - \frac{k_2}{k_1}S_1)X_2 \end{cases} \quad (3)$$

considered in the positively invariant set $\{(X_1, X_2, S_1, T_2) \in \mathbb{R}_+^4 | T_2 \geq \frac{k_2}{k_1}S_1\}$

In these new variables, the measure S_λ is rewritten as $S_\lambda = S_1 + \lambda S_2 = (1 - \lambda \frac{k_2}{k_1})S_1 + \lambda T_2$.

We will now impose a condition that we will call ‘‘regulability’’: this condition makes sure that, whatever the level $\bar{S}_\lambda \leq S_{\lambda max}$ that is regulated, there corresponds an equilibrium for system (3).

Let us pick \bar{S}_λ ; to an equilibrium satisfying $S_\lambda = \bar{S}_\lambda$ should correspond a constant dilution $\bar{D} > 0$. From the $\dot{X}_i = 0$ equations, we see that such an equilibrium should satisfy:

$$\mu_1(\bar{S}_1) = \mu_2\left(\frac{\bar{S}_\lambda - \bar{S}_1}{\lambda}\right) > 0$$

This potentially results in several values of $\bar{S}_1 > 0$ for our equilibrium, and corresponding values of \bar{D} .

Introducing this into the $\dot{S}_1 = \dot{T}_2 = 0$ equations, we obtain

$$\begin{aligned} 0 &= (S_{1in} - \bar{S}_1) - k_1\alpha\bar{X}_1 \\ 0 &= (T_{2in} - \bar{T}_2) - k_3\alpha\bar{X}_2 \end{aligned}$$

Isolating \bar{X}_1 and \bar{X}_2 , we get:

$$\begin{aligned} \bar{X}_1 &= \frac{S_{1in} - \bar{S}_1}{k_1\alpha} \\ \bar{X}_2 &= \frac{T_{2in} - \bar{T}_2}{k_3\alpha} \end{aligned}$$

At the equilibrium, \bar{X}_1 and \bar{X}_2 should be positive. Noticing that $\bar{S}_1 \leq \bar{S}_\lambda < S_{\lambda max}$ and $\lambda\bar{T}_2 \leq \bar{S}_\lambda < S_{\lambda max}$, it suffices to impose

$$S_{\lambda max} < \min(S_{1in}, \lambda T_{2in}) = \min\left(S_{1in}, \frac{\lambda k_2}{k_1} S_{1in} + \lambda S_{2in}\right) \quad (4)$$

to have \bar{X}_1 and \bar{X}_2 positive at any equilibrium having $\bar{S}_\lambda < S_{\lambda max}$. This assumption also forces $S_{\lambda max} < S_{\lambda in}$; it is reasonable, as we want to bring pollution to a lower level than its initial value.

Bounded control The control variable is the dilution rate, so that it must be non-negative, and it cannot be arbitrarily high. There is an a priori upper-bound on the maximal flow-rate D_{max} due to the physical constraint associated to the pumping mechanism. This bound can be seen as a given data, but it can also be seen a design parameter (a different choice of input valve can give a different value of upper-bound for D_{max}). On the other hand, the minimal value of the flow-rate is, theoretically, zero; however, in the industrial environment, the output of the industrial plant that produces the waste cannot be totally stopped, it is lower-bounded by some $D_{min} > 0$. We will design a controller that satisfies both these bounds.

For security reasons, we impose the following assumption

$$D_{max} < \frac{\min(\mu_1(S_{1in}), \mu_2(S_{2in}), \mu_2(T_{2in}))}{\alpha} \quad (5)$$

This assumption is made to avoid wash-out of the reactor. Indeed, if X_1 converges to 0, the \dot{S}_1 equation indicates that S_1 has to converge to S_{1in} , which means that the \dot{X}_1 equation converges to

$$\dot{X}_1 = (\mu_1(S_{1in}) - \alpha D)X_1 > 0$$

because of (5). No convergence of X_1 to 0 can then take place.

On the other hand, if X_2 converges to 0, the \dot{T}_2 equation indicates that T_2 converges to T_{2in} which means that the \dot{X}_2 equation converges to

$$\dot{X}_2 = \left(\mu_2\left(T_{2in} - \frac{k_2}{k_1}S_1\right) - \alpha D\right)X_2$$

It is easily seen that S_1 belongs to $[0, S_{1in}]$ after a finite time, so that $T_{2in} - \frac{k_2}{k_1}S_1$ then belongs to $[S_{2in}, T_{2in}]$. The growth rate μ_2 is then larger than $\min(\mu_2(S_{2in}), \mu_2(T_{2in})) > \alpha D_{max} > \alpha D$, so that $\dot{X}_2 > 0$ and no convergence of X_2 to zero is possible.

To summarize this section, we impose the following assumption in order to force a natural decrease of the pollution level when the input flow is stopped (2), make sure that there exists an equilibrium corresponding to the desired pollution level (4), and avoid wash-out of the reactor (5):

Assumption 1 *The parameters satisfy the following three inequalities*

$$\lambda < \frac{k_1}{k_2}$$

$$S_{\lambda max} < \min(S_{1in}, \lambda T_{2in}) = \min(S_{1in}, \frac{\lambda k_2}{k_1} S_{1in} + \lambda S_{2in})$$

$$D_{max} < \frac{\min(\mu_1(S_{1in}), \mu_2(S_{2in}), \mu_2(T_{2in}))}{\alpha}$$

2.1.2 Boundedness of the states

There exist $S_{1min}, T_{2min} > 0$ such that, for any choice of controller $D_{min} \leq D(X_1, S_1, X_2, S_2) \leq D_{max}$ and for any initial condition in the positive orthant $((X_1(0), S_1(0), X_2(0), S_2(0)) \in \mathbb{R}_+^4)$, there exists a finite time $T > 0$ after which the following four inequalities are valid:

$$S_{1in} < k_1 X_1(t) + S_1(t) < \frac{S_{1in}}{\alpha} \quad (6)$$

$$T_{2in} < k_3 X_2(t) + T_2(t) < \frac{T_{2in}}{\alpha} \quad (7)$$

$$S_{1min} < S_1(t) < S_{1in} \quad (8)$$

$$T_{2min} < T_2(t) < T_{2in} \quad (9)$$

for all $t \geq T$.

These inequalities are a consequence of the differentiation of the concerned quantities. The upper bound of inequality (6) is obtained from the following differentiation

$$\begin{aligned} \frac{d}{dt}(k_1 X_1 + S_1) &= k_1 \mu_1(S_1) X_1 - k_1 \alpha D X_1 + D(S_{1in} - S_1) - k_1 \mu_1(S_1) X_1 \\ &= D S_{1in} - \alpha D(k_1 X_1 + S_1) - (1 - \alpha) D S_1 \end{aligned} \quad (10)$$

$$\leq \alpha D \left(\frac{S_{1in}}{\alpha} - (k_1 X_1 + S_1) \right) \quad (11)$$

If $k_1 X_1(0) + S_1(0) \leq \frac{S_{1in}}{\alpha}$, the last inequality imposes that it stays valid. On the other hand, if $k_1 X_1(0) + S_1(0) > \frac{S_{1in}}{\alpha}$, this last inequality imposes that $\frac{d}{dt}(k_1 X_1 + S_1) < 0$ (because $D \geq D_{min}$), so that, either $k_1 X_1(t) + S_1(t)$ reaches $\frac{S_{1in}}{\alpha}$ in finite time, or it converges towards $\frac{S_{1in}}{\alpha}$ in infinite time. In the latter case, convergence then takes place towards the subset of $k_1 X_1 + S_1 = \frac{S_{1in}}{\alpha}$ inside which $\frac{d}{dt}(k_1 X_1 + S_1) = 0$. From (10), we see that this set is characterized by $S_1 = 0$. However, in $S_1 = 0$, we have $\dot{S}_1 = D S_{in} > D_{min} S_{in} > 0$, so that, no convergence towards $S_1 = 0$ can take

place. The value of $k_1X_1(t) + S_1(t)$ therefore reaches $\frac{S_{1in}}{\alpha}$ in finite time, and stays inferior or equal to that value for all future times (the strict inequality still needs to be shown). Also, we can deduce the lower bound in (6) from

$$\begin{aligned}\frac{d}{dt}(k_1X_1 + S_1) &= k_1\mu_1(S_1)X_1 - k_1\alpha DX_1 + D(S_{1in} - S_1) - k_1\mu_1(S_1)X_1 \\ &= DS_{1in} - D(k_1X_1 + S_1) + k_1(1 - \alpha)DX_1 \\ &\geq D(S_{1in} - (k_1X_1 + S_1))\end{aligned}$$

If $k_1X_1(0) + S_1(0) \geq S_{1in}$, the last inequality imposes that it stays valid. On the other hand, if $k_1X_1(0) + S_1(0) < S_{1in}$, this last inequality imposes that $\frac{d}{dt}(k_1X_1 + S_1) > 0$ (because $D \geq D_{min}$), so that, either $k_1X_1(t) + S_1(t)$ reaches S_{1in} in finite time, or it converges towards S_{1in} in infinite time. In the latter case, convergence then takes place towards the subset of $k_1X_1 + S_1 = S_{1in}$ inside which $\frac{d}{dt}(k_1X_1 + S_1) = 0$. We see that this set is characterized by $X_1 = 0$ (and $S_1 = S_{1in}$). However, if $X_1(0) > 0$ (so that $X_1(t) > 0$ for all $t \geq 0$), we have $\mu_1(S_1) > \alpha D$ when S_1 converges towards S_{1in} because of the security condition in Assumption 1; this implies $\dot{X}_1 > 0$, when S_1 approaches S_{1in} , and no convergence towards the hyperplane characterized by $(X_1, S_1) = (0, S_{1in})$ is possible. Therefore, the value of $k_1X_1(t) + S_1(t)$ reaches S_{1in} in finite time. Because $\frac{d}{dt}(k_1X_1 + S_1) > 0$ at that moment, we see that that we have $k_1X_1(t) + S_1(t) > S_{1in}$ for all future times.

The (non strict) upper bound in (7) comes from a similar treatment of

$$\begin{aligned}\frac{d}{dt}(k_3X_2 + T_2) &= D(T_2 - T_{2in}) - k_3\alpha DX_2 \\ &= DT_{2in} - \alpha D(k_3X_2 + T_2) - (1 - \alpha)DT_2 \\ &\leq \alpha D\left(\frac{T_{2in}}{\alpha} - (k_3X_2 + T_2)\right)\end{aligned}$$

On the other hand, the lower bound of (7) is derived from

$$\begin{aligned}\frac{d}{dt}(k_3X_2 + T_2) &= D(T_2 - T_{2in}) - k_3\alpha DX_2 \\ &= DT_{2in} - D(k_3X_2 + T_2) + (1 - \alpha)Dk_3X_2 \\ &\geq D(T_{2in} - (k_3X_2 + T_2))\end{aligned}$$

If $k_3X_2(0) + T_2(0) \geq T_{2in}$, the last inequality imposes that it stays valid. On the other hand, if $k_3X_2(0) + T_2(0) < T_{2in}$, this last inequality imposes that $\frac{d}{dt}(k_3X_2 + T_2) > 0$ (because $D \geq D_{min}$), so that, either $k_3X_2(t) + T_2(t)$ reaches T_{2in} in finite time, or it converges towards T_{2in} in infinite time. In the latter case, convergence then takes place towards the subset of $k_3X_2 + T_2 = T_{2in}$ inside which $\frac{d}{dt}(k_3X_2 + T_2) = 0$. We see that this set is characterized by $X_2 = 0$ (and $T_2 = T_{2in}$). However, if $X_2(0) > 0$ (so that $X_2(t) > 0$ for all $t \geq 0$), we have $\mu_2(T_2 - \frac{k_2}{k_1}S_1) > \alpha D$ when T_2 converges towards T_{2in} because of Assumption 1; indeed, $S_1 \in [0, S_{1in}]$, so that the argument of μ_2 belongs to the interval $[T_{2in} - \frac{k_2}{k_1}S_{1in}, T_{2in}] = [S_{2in}, T_{2in}]$ (at the limit) when T_2 converges towards T_{2in} . Therefore, $\mu_2(T_2 - \frac{k_2}{k_1}S_1) > \min(\mu_2(S_{2in}), \mu_2(T_{2in})) > \alpha D_{max} \geq \alpha D$. This implies $\dot{X}_2 > 0$, when T_2 approaches T_{2in} , and no convergence towards the hyperplane characterized by $(X_2, T_2) = (0, T_{2in})$ is possible. Therefore, the value of $k_3X_2(t) + T_2(t)$ reaches T_{2in} in finite time. Because $\frac{d}{dt}(k_3X_2 + T_2) > 0$ at that moment, we see that that we have $k_3X_2(t) + T_2(t) > T_{2in}$ for all future times.

The differential equation steering S_1 yields

$$\dot{S}_1 = D(S_{1in} - S_1) - k_1\mu_1(S_1)X_1 \leq D(S_{1in} - S_1)$$

From the last inequality, we see that, if $S_1(0) \leq S_{1in}$, inequality (8) stays satisfied for all future times. On the other hand, if $S_1(0) > S_{1in}$, we have $\dot{S}_1 < 0$ because $D \geq D_{min} > 0$. Therefore, either S_1 reaches S_{1in} in finite time or S_1 converges towards S_{1in} in infinite time. In the latter case, the solution of the system must converge towards the subset of the region $S_1 = S_{1in}$ where $\dot{S}_1 = 0$. This subset is characterized by $X_1 = 0$. We have already shown that such a convergence was not possible. The solutions therefore reach $S_1 = S_{1in}$ in finite time, where $\dot{S}_1 < 0$, so that the right-hand side of (8) is proven. The left-hand side of this inequality comes from the use of (6), which implies that $X_1(t) < \frac{S_{1in}}{k_1\alpha}$ after a finite time. We then have

$$\dot{S}_1 = D(S_{1in} - S_1) - k_1\mu_1(S_1)X_1 > D_{min}(S_{1in} - S_1) - k_1\mu_1(S_1)\frac{S_{1in}}{k_1\alpha}$$

We see that, when S_1 is small, we have $\dot{S}_1 > 0$. Defining S_{1min} as $1 - \epsilon$ times the smallest $S_1 > 0$ such that $D_{min}(S_{1in} - S_1) - k_1\mu_1(S_1)\frac{S_{1in}}{k_1\alpha} = 0$, we obtain the left-hand side of (8) (for some $\epsilon > 0$ small).

This helps us show that the upper-bound of (6) is strict. Indeed, when $k_1X_1 + S_1 = \frac{S_{1in}}{\alpha}$, we have

$$\frac{d}{dt}(k_1X_1 + S_1) = DS_{1in} - \alpha D(k_1X_1 + S_1) - (1 - \alpha)DS_1 > -(1 - \alpha)S_{1min} > 0$$

The upper-bound of (9) is obtained in the same way from the \dot{T}_2 equation. The lower-bound of (9) is derived from

$$\begin{aligned} \dot{T}_2 &= D(T_{2in} - T_2) - k_3\mu_2(T_2 - \frac{k_2}{k_1}S_1)X_2 \\ &> D_{min}(T_{2in} - T_2) - k_3 \max_{t_2 \in [T_2 - \frac{k_2}{k_1}S_{1in}, T_2 - \frac{k_2}{k_1}S_{1min}]} \mu_2(t_2) \frac{S_{2in}}{k_3\alpha} \end{aligned}$$

We see that, when T_2 is small, we have $\dot{T}_2 > 0$. Defining T_{2min} as $1 - \epsilon$ times the smallest $T_2 > 0$ such that

$$D_{min}(T_{2in} - T_2) - k_3 \max_{t_2 \in [T_2 - \frac{k_2}{k_1}S_{1in}, T_2 - \frac{k_2}{k_1}S_{1min}]} \mu_2(t_2) \frac{S_{2in}}{k_3\alpha} = 0$$

we obtain the left-hand side of (9).

We will complete this overview of the constraints by the following observation: For any X_1 , the constraints (6) and (8) imply that $\max(S_{1in} - k_1X_1, S_{1min}) < S_1 < \min(\frac{S_{1in}}{\alpha} - k_1X_1, S_{1in})$. Defining X_{1min} as the maximal value such that $\mu_1(\max(S_{1in} - k_1X_1, S_{1min})) = (1 + \epsilon)\alpha D_{max}$ (for some small ϵ), we see that, for $X_1 \leq X_{1min}$, we have $\dot{X}_1 > 0$, so that $X_1 > X_{1min}$ after a finite time.

Inequalities (6)-(9) ensure boundedness of the four states of the system.

Lemma 1 Let any initial condition $(X_1(0), X_2(0), S_1(0), S_2(0))$ belonging to \mathbb{R}_+^4 , then, for given constants S_{1in}, S_{2in} such that Assumption 1 is satisfied, there exists a time $T > 0$ such that, for all $t \geq T$, we have

$$\begin{aligned} X_{1min} &< X_1(t) < \frac{S_{1in}}{k_1\alpha} \\ 0 &< X_2(t) < \frac{T_{2in}}{k_3\alpha} \\ S_{1min} &< S_1(t) < S_{1in} \\ T_{2min} &< T_2(t) < T_{2in} \end{aligned}$$

along the solution of (1) for any choice of $D(t) \in [D_{min}, D_{max}]$.

2.1.3 Control design

In this text, we choose a simple proportional controller in the form

$$D = \frac{D_{max} - D_{min}}{2} \left(1 + \text{sat} \left(\frac{S_{\lambda max} + S_{\lambda min} - 2S_{\lambda}}{S_{\lambda max} - S_{\lambda min}} \right) \right) + D_{min} \quad (12)$$

where $\text{sat}(s) = \frac{s}{\max(|s|, 1)}$. As stated in Objective 1, this controller is not designed to regulate S_{λ} at a prespecified value \bar{S}_{λ} , but rather to ensure attractivity and invariance of the region of the state space where S_{λ} belongs to an interval $[S_{\lambda min}, S_{\lambda max}]$. Such a controller should be more robust than a controller aimed at exactly regulating the output. The main tuning parameters of this controller are the constants D_{max} and $S_{\lambda min}$ (though D_{max} might not be picked arbitrarily large in the actual plant due to physical constraints).

This controller is based on the following philosophy:

- (i) if $S_{\lambda} \geq S_{\lambda max}$ then the flow is minimal: it prevents the pollution from leaving the plant in too large an amount; the pollution is lowered inside the plant and the bacteria grow in order to face the higher depollution requirement;
- (ii) if $S_{\lambda} \leq S_{\lambda min}$ then the flow is allowed to be maximal because the pollution level is low enough to be certain that this maximal flow will not drive the system into the region where the pollution is too high;
- (iii) if $S_{\lambda min} < S_{\lambda} < S_{\lambda max}$ then the controller is linear and built such that it is continuous at the boundaries of this region.

The description of the controller as (i)-(ii)-(iii) allows for the separate description of the controlled system (1)-(12) in the three corresponding regions, that we will name Ω_1 , Ω_2 , and Ω_3 , respectively:

Region Ω_1 : $D = D_{min}$ The region Ω_1 is defined as

$$\Omega_1 = \{(X_1, X_2, S_1, S_2) \in (\mathbb{R}^+)^4 \mid S_1 + \lambda S_2 \geq S_{\lambda max}\}$$

In this region, where $S_{\lambda} \geq S_{\lambda max}$, the flow rate is rendered minimal to limit the outflow of pollutants. System (1) can be rewritten as

$$\begin{cases} \dot{X}_1 &= (\mu_1(S_1) - \alpha D_{min})X_1 \\ \dot{X}_2 &= (\mu_2(S_2) - \alpha D_{min})X_2 \\ \dot{S}_1 &= D_{min}(S_{1in} - S_1) - k_1\mu_1(S_1)X_1 \\ \dot{S}_2 &= D_{min}(S_{2in} - S_2) + k_2\mu_1(S_1)X_1 - k_3\mu_2(S_2)X_2 \end{cases} \quad (13)$$

This system can be analyzed as a cascade system between the (X_1, S_1) subsystem and the (X_2, S_2) subsystem. For any constant $D_{min} < \frac{\mu_{1max}}{\alpha}$, the state of the (X_1, S_1) subsystem globally converges to the non-trivial equilibrium $(\bar{X}_1, \bar{S}_1) = \left(\frac{S_{1in} - \mu_1^{-1}(\alpha D_{min})}{k_1\alpha}, \mu_1^{-1}(\alpha D_{min}) \right)$. Also, the smaller D_{min} is, the smaller \bar{S}_1 is. Because the solutions of the whole system are bounded, we know that the

behavior of the whole system (13) can be deduced from the behavior of the (X_2, S_2) subsystem on the manifold $(X_1, S_1) = (\bar{X}_1, \bar{S}_1)$. This system is

$$\begin{cases} \dot{X}_2 &= (\mu_2(S_2) - \alpha D_{min})X_2 \\ \dot{S}_2 &= D_{min}(S_{2in} + \frac{k_2}{k_1}(S_{1in} - \mu_1^{-1}(\alpha D_{min})) - S_2) - k_3\mu_2(S_2)X_2 \end{cases} \quad (14)$$

Generically, this system has two non-trivial equilibria because μ_2 is of Haldane type; the equilibria are characterized by the two values of S_2 that are such that $\mu_2(S_2) = \alpha D_{min}$ ($S_2^m < S_2^* < S_2^M$, see Figure 1 for an illustration of these values). It is apparent, on the figure, that S_2^M is increasing and S_2^m decreasing when D_{min} is decreasing. Independently of the choice of D_{min} , the \dot{S}_2 equation in (14) clearly shows that $S_2 \leq S_{2in} + \frac{k_2}{k_1}S_{1in} = T_{2in}$ after a finite time. Also, if we take D_{min} small enough, we can have $S_2^M > T_{2in}$, so that no convergence to the equilibrium corresponding to $S_2 = S_2^M$ can take place, and all solutions converge towards the equilibrium corresponding to $S_2 = S_2^m$. This equilibrium is characterized by $\bar{S}_\lambda = \bar{S}_1 + \lambda S_2^m = \mu_1^{-1}(\alpha D_{min}) + \lambda S_2^m$, which can

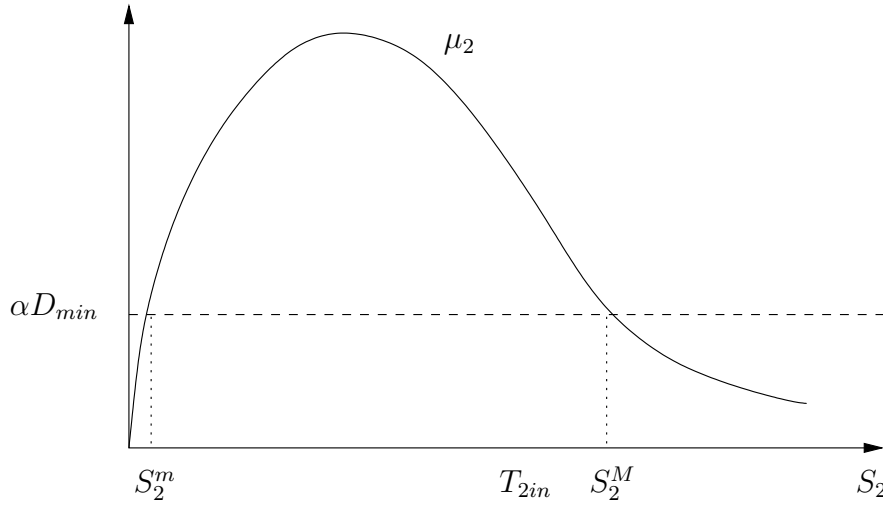


Figure 1: Illustration of the possibility of taking D_{min} small enough in order to have a single root of $\mu_2(S_2) = \alpha D_{min}$ inside the region $S_2 \leq T_{2in}$

be made as small as we want by reducing D_{min} . We then make the following assumption

Assumption 2 $D_{min} > 0$ is taken small enough so that $S_2^M > T_{2in}$ and $\bar{S}_1 + \lambda S_2^m < S_{\lambda max}$.

This assumption ensures that system (13) has a single equilibrium, and that this equilibrium lies in the region where $S_\lambda < S_{\lambda max}$. We can show that this equilibrium is attractive for all initial conditions for system (13), so that we know that $S_\lambda = S_{\lambda max}$ is reached in finite time. We have then shown attractivity of $\Omega_2 \cup \Omega_3$. We now have to show invariance of this set. On its border, (2) becomes:

$$\dot{S}_\lambda = D_{min}(S_{\lambda in} - S_{\lambda max}) - (k_1 - \lambda k_2)\mu_1(S_1)X_1 - \lambda k_3\mu_2(S_2)X_2$$

We will show that, in the region defined by the constraints (6)-(9), we have $(k_1 - \lambda k_2)\mu_1(S_1)X_1 + \lambda k_3\mu_2(S_2)X_2 \geq M > 0$ when $S_\lambda = S_{\lambda max}$. This shows that, for $D_{min} > 0$ small enough $\dot{S}_\lambda < 0$ when $S_\lambda = S_{\lambda max}$.

We want to evaluate

$$\begin{aligned}
M &= \min && (k_1 - \lambda k_2)\mu_1(S_1)X_1 + \lambda k_3\mu_2(S_2)X_2 \\
\text{s.t.} &&& S_1 + \lambda S_2 = S_{\lambda max} \\
&&& S_{1in} \leq k_1 X_1 + S_1 \leq \frac{S_{1in}}{\alpha} \\
&&& T_{2in} \leq k_3 X_2 + S_2 + \frac{k_2}{k_1} S_1 < \frac{T_{2in}}{\alpha}
\end{aligned}$$

We can eliminate S_2 from $(k_1 - \lambda k_2)\mu_1(S_1)X_1 + \lambda k_3\mu_2(S_2)X_2$ by replacing it with $\frac{S_{\lambda max} - S_1}{\lambda}$. Also, the other two constraints indicate that

$$X_1 \geq \frac{S_{1in} - S_1}{k_1}$$

and

$$\begin{aligned}
X_2 &\geq \frac{T_{2in} - S_2 - \frac{k_2}{k_1} S_1}{k_3} \\
&= \frac{T_{2in} - \frac{S_{\lambda max} - S_1}{\lambda} + (\frac{1}{\lambda} - \frac{k_2}{k_1}) S_1}{k_3}
\end{aligned}$$

Both those lower bounds are positive because of Assumption 1. We can then say that

$$\begin{aligned}
M \geq N &= \min && (k_1 - \lambda k_2)\mu_1(S_1) \frac{S_{1in} - S_1}{k_1} \\
&&& + \mu_2\left(\frac{S_{\lambda max} - S_1}{\lambda}\right) (\lambda T_{2in} - S_{\lambda max} + (1 - \frac{\lambda k_2}{k_1}) S_1) \\
\text{s.t.} &&& 0 \leq S_1 \leq S_{\lambda max}
\end{aligned} \tag{15}$$

It is easily seen that $N > 0$ by noting that both terms cannot be equal to zero at the same time. We then see that, as long as $D_{min} \leq \frac{N}{S_{\lambda in} - S_{\lambda max}}$, the region $\Omega_2 \cup \Omega_3$ is attractive and invariant. We then state the following assumption

Assumption 3 *The minimal dilution rate D_{min} satisfies the following constraint*

$$D_{min} \leq \frac{N}{S_{\lambda in} - S_{\lambda max}}$$

where N is defined in (15).

We then have the following result:

Lemma 2 Under Assumptions 1, 2, and 3, there exists a finite time T after which the region $\Omega_2 \cup \Omega_3$ is attractive and invariant for system (1) with the controller (12).

This lemma ensures that the depollution objective is achieved by the controller; the pollution level will always be kept below $S_{\lambda max}$ once the controller has forced the system into that region. We will now study the behavior of the system in the other two regions and check if Objective 1 is achieved.

Region Ω_2 : $D = D_{max}$ The region Ω_2 is defined as

$$\Omega_2 = \{(X_1, X_2, S_1, S_2) \in (\mathbb{R}^+)^4 \mid S_1 + \lambda S_2 \leq S_{\lambda min}\}$$

In this region, where $S_\lambda \leq S_{\lambda min}$, system (1) can be rewritten as:

$$\begin{cases} \dot{X}_1 &= (\mu_1(S_1) - \alpha D_{max})X_1 \\ \dot{X}_2 &= (\mu_2(S_2) - \alpha D_{max})X_2 \\ \dot{S}_1 &= D_{max}(S_{1in} - S_1) - k_1\mu_1(S_1)X_1 \\ \dot{S}_2 &= D_{max}(S_{2in} - S_2) + k_2\mu_1(S_1)X_1 - k_3\mu_2(S_2)X_2 \end{cases} \quad (16)$$

In Ω_2 , we only need to check the evolution of $S_\lambda(t)$, which follows the equation (2):

$$\dot{S}_\lambda = D_{max}(S_{\lambda in} - S_\lambda) - (k_1 - \lambda k_2)\mu_1(S_1)X_1 - \lambda k_3\mu_2(S_2)X_2$$

so that, on the border of the region, it satisfies:

$$\dot{S}_\lambda = D_{max}(S_{\lambda in} - S_{\lambda min}) - (k_1 - \lambda k_2)\mu_1(S_1)X_1 - \lambda k_3\mu_2(S_2)X_2$$

From Lemma 1, we know that there exists a finite time $T > 0$ after which $X_1(t) \leq \frac{S_{1in}}{k_1\alpha}$ and $X_2(t) \leq \frac{T_{2in}}{k_3\alpha}$. We then have

$$\dot{S}_\lambda \geq D_{max}(S_{\lambda in} - S_{\lambda min}) - (k_1 - \lambda k_2) \left[\max_{S_1 \leq S_{\lambda min}} \mu_1(S_1) \right] \frac{S_{1in}}{k_1\alpha} - \lambda k_3 \left[\max_{S_2 \leq \frac{S_{\lambda min}}{\lambda}} \mu_2(S_2) \right] \frac{T_{2in}}{k_3\alpha}$$

for all $S_\lambda \leq S_{\lambda min}$. In order to have \dot{S}_λ always positive, we impose the following assumption

Assumption 4 *Suppose that*

$$D_{max} > \frac{(k_1 - \lambda k_2)\mu_1(S_{\lambda min})\frac{S_{1in}}{k_1\alpha} + \lambda k_3 \left[\max_{S_2 \leq \frac{S_{\lambda min}}{\lambda}} \mu_2(S_2) \right] \frac{T_{2in}}{k_3\alpha}}{S_{\lambda in} - S_{\lambda min}} \quad (17)$$

This assumption can be satisfied by picking the parameter D_{max} large enough or the free parameter $S_{\lambda min}$ small enough. From this expression, we deduce the following lemma:

Theorem 1 *Assumptions 1-4 ensure that there exists a finite time after which Objective 1 is satisfied by system (1) with controller (12).*

This theorem is a consequence of the observations made prior to its statement, which show that all solutions have to leave Ω_2 after a finite time, and of Lemma 2 which shows the same thing for Ω_1 . All solutions then converge to the invariant set Ω_3 inside which the depollution objective is achieved. Note that attractivity and invariance of the region of interest is not directly ensured: the solutions first have to converge to the region where (6)-(9) is satisfied (and we have shown that this takes place in finite time), and then we know that Ω_3 is attractive and invariant.

Remark 1 *Taking a look back at all the assumptions, we see that λ and $S_{\lambda max}$ are data given by the depollution norms. With the identified parameters of the experimental plant, λ satisfies the constraint described in Assumption 1. If the value of $S_{\lambda max}$ given by the depollution norm does not satisfy Assumption 1, we take a smaller value in our controller design; this results in a controller that forces the regulated system to satisfy a constraint that is stronger than the depollution norm. The last constraint of Assumption 1 is a security constraint that limits the tolerated value of D_{max} (to avoid wash-out of the bacteria). D_{max} also has to be smaller than the maximal value that the input valve can let through.*

Once these three parameters are fixed, it then suffices to take D_{min} and $S_{\lambda min}$ small enough to satisfy Assumptions 2, 3, and 4.

We have to be very careful with the implementation of this part of the controller because, if, for some reason, the security constraint of Assumption 1 is not satisfied, and we have D_{max} large, the constant control D_{max} would lead to a wash-out of the bacteria. Luckily, even if D_{max} is too large, the structure of the complete controller (12) prevents this wash-out from actually occurring.

By the analysis of the behavior of the system in regions Ω_1 and Ω_2 , we have shown that the region Ω_3 where $S_{\lambda min} \leq S_\lambda \leq S_{\lambda max}$ is attractive and invariant. The depollution objective is achieved. However, we would like to know what actually occurs inside the region Ω_3 .

Region Ω_3 : $D = D_{min} + (D_{max} - D_{min}) \frac{S_{\lambda max} - S_\lambda}{S_{\lambda max} - S_{\lambda min}}$ The region Ω_3 is defined as

$$\Omega_3 = \{(X_1, X_2, S_1, S_2) \in (\mathbb{R}^+)^4 \mid S_{\lambda min} \leq S_1 + \lambda S_2 \leq S_{\lambda max}\}$$

In this region, where $S_{\lambda min} \leq S_\lambda \leq S_{\lambda max}$, system (1) can be rewritten as:

$$\begin{cases} \dot{X}_1 &= \left(\mu_1(S_1) - \alpha \left(D_{min} + (D_{max} - D_{min}) \frac{S_{\lambda max} - S_\lambda}{S_{\lambda max} - S_{\lambda min}} \right) \right) X_1 \\ \dot{X}_2 &= \left(\mu_2(S_2) - \alpha \left(D_{min} + (D_{max} - D_{min}) \frac{S_{\lambda max} - S_\lambda}{S_{\lambda max} - S_{\lambda min}} \right) \right) X_2 \\ \dot{S}_1 &= \left(D_{min} + (D_{max} - D_{min}) \frac{S_{\lambda max} - S_\lambda}{S_{\lambda max} - S_{\lambda min}} \right) (S_{1in} - S_1) - k_1 \mu_1(S_1) X_1 \\ \dot{S}_2 &= \left(D_{min} + (D_{max} - D_{min}) \frac{S_{\lambda max} - S_\lambda}{S_{\lambda max} - S_{\lambda min}} \right) (S_{2in} - S_2) + k_2 \mu_1(S_1) X_1 \\ &\quad - k_3 \mu_2(S_2) X_2 \end{cases} \quad (18)$$

We will study the equilibria of this system. It is easily seen that this region does not contain any wash-out equilibrium. Indeed, if $\bar{X}_1 = 0$ at the equilibrium, the $\dot{X}_1 = 0$ equation is satisfied, and the $\dot{S}_1 = 0$ equation imposes $S_1 = S_{1in}$ (because $D > 0$), which is not possible because, inside Ω_3 , we have $S_1 \leq S_\lambda \leq S_{\lambda max} < S_{1in}$. On the other hand, if $\bar{X}_2 = 0$ (so that $\dot{X}_2 = 0$), the $\dot{T}_2 = 0$ equation imposes $T_2 = T_{2in}$ (see (3)), which is not possible because, inside Ω_3 , we have $T_2 \leq \frac{S_\lambda}{\lambda} \leq \frac{S_{\lambda max}}{\lambda} < T_{2in}$.

Considering the cases where $\bar{X}_1 \neq 0$ and $\bar{X}_2 \neq 0$, we must have $\mu_1(S_1) = \mu_2(S_2) = \alpha D_{min} + \alpha (D_{max} - D_{min}) \frac{S_{\lambda max} - S_1 - \lambda S_2}{S_{\lambda max} - S_{\lambda min}}$. We then have:

$$S_1 = \mu_1^{-1}(\mu_2(S_2)) = \nu(S_2)$$

In order to ensure continuity of function ν , we must have the following (which is satisfied with the identified data):

$$\mu_{1max} > \mu_{2max} \frac{\sqrt{K_{I_2}}}{\sqrt{K_{I_2}} + 2\sqrt{K_{S_2}}}$$

With this inequality, $\nu(S_2)$ is strictly increasing from $S_2 = 0$ to $S_2 = \sqrt{K_{S_2} K_{I_2}}$ and strictly decreasing afterwards (so that it is bounded: $\nu(S_2) \leq \mu_1^{-1}(\mu_2(\sqrt{K_{S_2} K_{I_2}})) = \nu_{max}$). Also, we have $\lim_{S_2 \rightarrow +\infty} \nu(S_2) = 0$.

If the inequality is not satisfied, ν is not defined in the interval $[S_{2min}, S_{2max}]$ where $\mu_2(S_2) \geq \mu_{1max}$. Also $\lim_{S_2 \rightarrow S_{2max}} \nu(S_2) = \lim_{S_2 \rightarrow S_{2min}} \nu(S_2) = +\infty$.

The following analysis is valid in both cases, if we define $S_2^* = \sqrt{K_{S_2} K_{I_2}}$ or $S_2^* = S_{2max}$ in the first or second case, respectively.

Defining

$$\begin{aligned}\zeta(S_2) &= \alpha D_{min} + \alpha(D_{max} - D_{min}) \frac{S_{\lambda max} - \nu(S_2) - \lambda S_2}{S_{\lambda max} - S_{\lambda min}} \\ &= \alpha \frac{D_{max} S_{\lambda max} - D_{min} S_{\lambda min} - (D_{max} - D_{min})(\nu(S_2) + \lambda S_2)}{S_{\lambda max} - S_{\lambda min}}\end{aligned}$$

the equilibria must also satisfy:

$$\mu_2(S_2) = \zeta(S_2) \quad (19)$$

In order to have a simple behavior to the system, we would like to have only one equilibrium in that family, that is only one root to (19). We present a simple way of ensuring that this equilibrium lies in the region where $\mu_2(S_2)$ is increasing. It consists in imposing a root in the in-

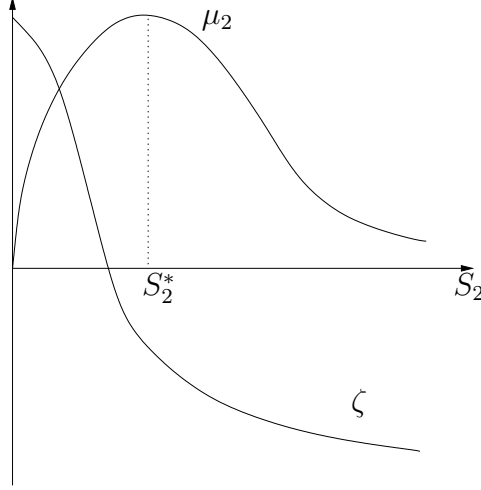


Figure 2: Illustration of the equality $\mu_2(S_2) = \zeta(S_2)$: $\zeta(S_2) < 0$ for all $S_2 > S_2^*$, so that $\mu_2(S_2) = \zeta(S_2)$ has a single root.

terval $[0, S_2^*]$, and preventing the presence of a root outside this interval (obviously, in the case where ν is not globally defined, no root can be found between S_{2min} and S_2^*). Observing that $\zeta(0) = \alpha \frac{D_{max} S_{\lambda max} - D_{min} S_{\lambda min}}{S_{\lambda max} - S_{\lambda min}} > 0$, that $\mu_2(0) = 0$, and that ζ is strictly decreasing and μ_2 strictly increasing on the interval $[0, S_2^*)$, (19) can have at most one root inside the interval. If $\zeta(S_2) < 0$ for all $S_2 \geq S_2^*$, it is easy to see that (19) has one root inside $[0, S_2^*)$ and no root outside this interval. This is illustrated on Figure 2.

This can be achieved by imposing $(D_{max} - D_{min})\lambda S_2 > D_{max} S_{\lambda max} - D_{min} S_{\lambda min}$ for $S_2 > S_2^*$, it suffices then to impose

$$\frac{D_{max} S_{\lambda max} - D_{min} S_{\lambda min}}{(D_{max} - D_{min})} < \lambda S_2^*$$

Note that this equality can always be satisfied by taking D_{min} small enough if we have the following assumption:

Assumption 5 *The maximal tolerated pollution level satisfies*

$$S_{\lambda max} < \lambda S_2^*$$

where S_2^* is either

- the value of S_2 that yields the maximum of μ_2 if $\mu_{1max} \geq \mu_{2max} \frac{\sqrt{K_{I_2}}}{\sqrt{K_{I_2}+2}\sqrt{K_{S_2}}}$
- the largest of the two values of S_2 such that $\mu(S_2) = \mu_{1max}$ otherwise

When $\lambda < 1$, this forces the system to stay in the region where the growth-rate of the methanogenesis is increasing. The value of $S_{\lambda max}$ is strongly constrained by the model.

The remaining two states at the equilibrium follow directly from the $\dot{S}_1 = \dot{S}_2 = 0$ equations. The exponential stability of this equilibrium could be proven by considering the Jacobian linearization of (18) around the equilibrium.

From this analysis, we have seen that the region characterized by $S_{\lambda min} < S_\lambda < S_{\lambda max}$ is globally attractive and invariant. This result is summarized in the following theorem, which complements Theorem 1

Theorem 2 *Assumptions 1-5 ensure that there exists a finite time after which Objective 1 is satisfied by system (1) with controller (12). Moreover, this system has a single equilibrium (which lies in Ω_3).*

2.1.4 Interval observation

Oftentimes, there is no online measurement of the COD: sporadic measurements are made with large time intervals between them. Based on those, on a knowledge of an interval inside which lies $S_{\lambda in}$ and on the methane gaseous flow-rate, it is possible to reconstruct an interval $[\underline{S}_\lambda(t), \bar{S}_\lambda(t)]$ inside which the signal $S_\lambda(t)$ lies:

$$\underline{S}_\lambda(t) \leq S_\lambda(t) \leq \bar{S}_\lambda(t) \text{ for all } t \geq 0$$

The width of this interval is very important to the result of the control problem: how can we ensure that the actual value of S_λ lies in the interval $[S_{\lambda min}, S_{\lambda max}]$ if we have an estimate that does not even have the accuracy of that interval? What do we do if $S_\lambda(t) > S_{\lambda max}$ and $S_\lambda(t) < S_{\lambda min}$? In that case, we will concentrate on the upper-bound and make sure that S_λ is always smaller than $S_{\lambda max}$ after a finite time, but some hysteresis will have to be introduced to avoid chattering. This leads to the following controller:

- (i) if $\bar{S}_\lambda \geq S_{\lambda max}$ and $\underline{S}_\lambda \geq S_{\lambda min}$ then the flow is set to its minimal value: $\bar{S}_\lambda \geq S_{\lambda max}$ implies that we might have $S_\lambda \geq S_{\lambda max}$, so that we must prevent the pollution from leaving the plant in too large an amount; the pollution is lowered inside the plant and the bacteria grow in order to face the higher depollution requirement ($D = D_{min}$);
- (i)' if $\bar{S}_\lambda \geq S_{\lambda max}$ and $\underline{S}_\lambda \leq S_{\lambda min}$, then $D = D_{min}$ for the same reason. However, some hysteresis is introduced by adding that $D = D_{min}$ is maintained as long as $\bar{S}_\lambda \geq \eta S_{\lambda max}$ (with $0 < \eta < 1$). Indeed, without this hysteresis, chattering could occur between this part of the controller and the part (ii) when \bar{S}_λ reaches $S_{\lambda max}$;
- (ii) if $\underline{S}_\lambda \leq S_{\lambda min}$ in situations other than those of case (i)', then the flow is allowed to be maximal ($D = D_{max}$);

(iii) if $S_{\lambda min} < \underline{S}_\lambda$ and $\bar{S}_\lambda < S_{\lambda max}$ and the controller is not in the hysteresis phase, then the controller is built such that it is continuous at the boundaries of this region; it takes the form:

$$D = \frac{D_{min}(\underline{S}_\lambda - S_{\lambda min}) + D_{max}(S_{\lambda max} - \bar{S}_\lambda)}{(S_{\lambda max} - S_{\lambda min}) - (\bar{S}_\lambda - \underline{S}_\lambda)}$$

The stability analysis of this controller is very similar to what was shown in the previous section. In particular, in the case where the interval $[\underline{S}_\lambda(t), \bar{S}_\lambda(t)]$ is smaller than the interval $[S_{\lambda min}, S_{\lambda max}]$, it can be shown that the interval $[S_{\lambda min}, S_{\lambda max}]$ is attractive and invariant after a finite time for $S(t)$. A more accurate analysis should be performed by introducing the dynamics of the actual observer in the system that we analyze.

2.1.5 Simulations

We have implemented controller (12) on model (1). For the simulations, we have used the parameters of the model that were given in Deliverable D3.1a. We then fixed the following “free” parameters as follows:

$$S_{\lambda max} = 2; S_{\lambda min} = 1.8; S_{1in} = 5; S_{2in} = 1; \lambda = 0.3; D_{max} = 0.4; D_{min} = 0.1.$$

As can be seen from these parameters, the purpose of the control design is here to steer S_λ into the interval $[1.8, 2]$ with a control effort lying in the interval $[0.1, 0.4]$. We have considered two sets of initial conditions.

The first set is $(S_1, S_2, X_1, X_2)(0) = (6, 2, 0.05, 0.05)$. This set is characterized by a very low biomass at the start and a high pollution level in the reactor ($S_\lambda(0) = 7.2$), mainly coming from the large amount of S_1 in the reactor. The dilution rate is then set at the minimal level during the first three days. As can be seen on Figure 3, this forces a decrease of the pollution level S_λ and of S_1 . Simultaneously, the biomass X_1 and X_2 quickly increase. After 4 days, the pollution level settles at the desired value, between $S_{\lambda min}$ and $S_{\lambda max}$, and the dilution rate also reaches a steady state. However, it is interesting to notice that this does not mean that the solution has reached its equilibrium. Indeed, between day 4 and day 30, we observe a continuing increase of X_1 and S_2 , coupled with a decrease of X_2 . After that, the equilibrium is reached. This phenomenon is also illustrated on Figure 4, where an (S_1, S_2) phase plane is plotted. It is seen that the solution enters the region Ω_3 (between the dotted lines), stays there for all future times while settling to the equilibrium.

The second set of initial conditions is $(S_1, S_2, X_1, X_2)(0) = (6, 2, 1, 1)$. It is characterized by a very high level of biomass, as well as pollution. As can be seen on Figure 5, the dilution rate is set at its minimal value for a very short time. A very fast decrease of S_λ then takes place, thanks to the high level of biomass. This decrease goes well below $S_{\lambda min}$, which means that the dilution rate is set at its maximal level. The (still) high level of biomass makes sure that the reactor can handle the maximal dilution rate until time $t = 18$, while maintaining a very low, but increasing, pollution level inside the plant. Simultaneously, the biomass decreases to values that correspond more to the requested amount of biomass to treat the given input pollution level. Finally S_λ reaches $S_{\lambda min}$ again and the dilution rate is reduced, so that it settles at its equilibrium value. On Figure 6, where an (S_1, S_2) phase plane is plotted, we see that the Ω_3 region is not directly invariant: the

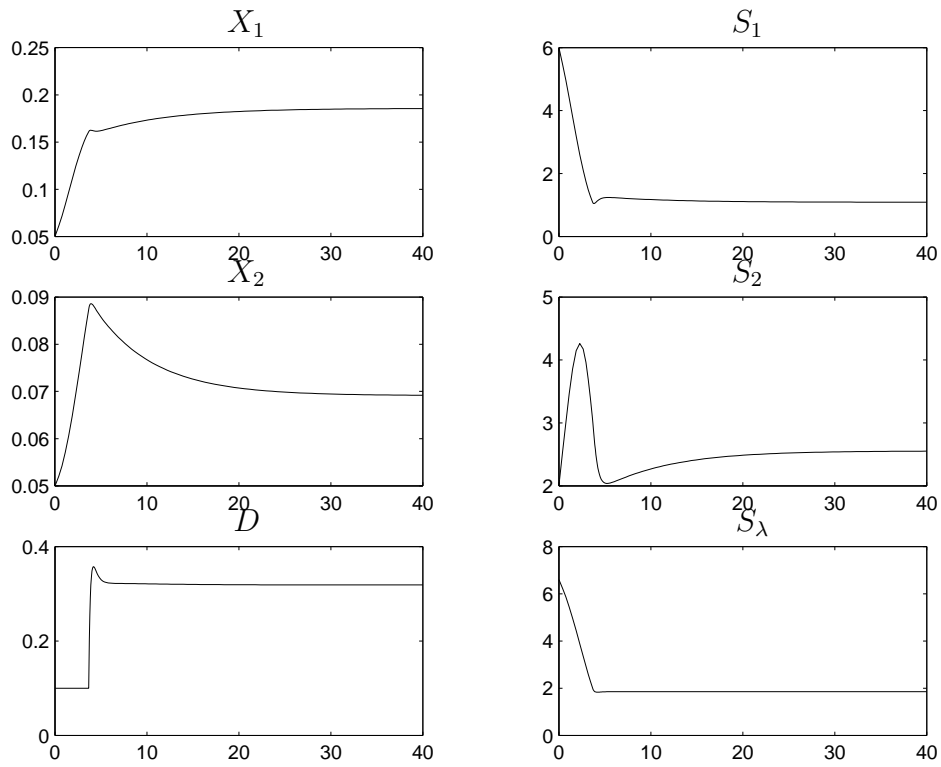


Figure 3: Time evolution of the states, control D , and output S_λ for the control system with the first set of initial conditions $(S_1, S_2, X_1, X_2)(0) = (6, 2, 0.05, 0.05)$

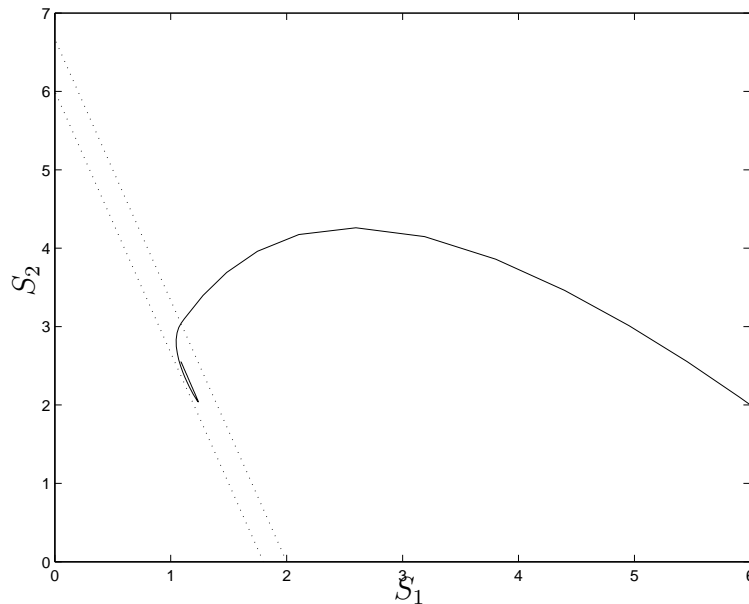


Figure 4: (S_1, S_2) phase plane for the control system with the first set of initial conditions $(S_1, S_2, X_1, X_2)(0) = (6, 2, 0.05, 0.05)$; the dotted lines represent the limits of region Ω_3

solution goes from $(S_1, S_2) = (6, 2)$ through Ω_3 into the region Ω_2 before entering Ω_3 again and settle to its equilibrium. Note that this is not in contradiction with Theorems 1 and 2: attractivity and invariance of the region Ω_3 in these theorems is only ensured after a finite time: the time that it takes for conditions (6)-(9) to be satisfied.

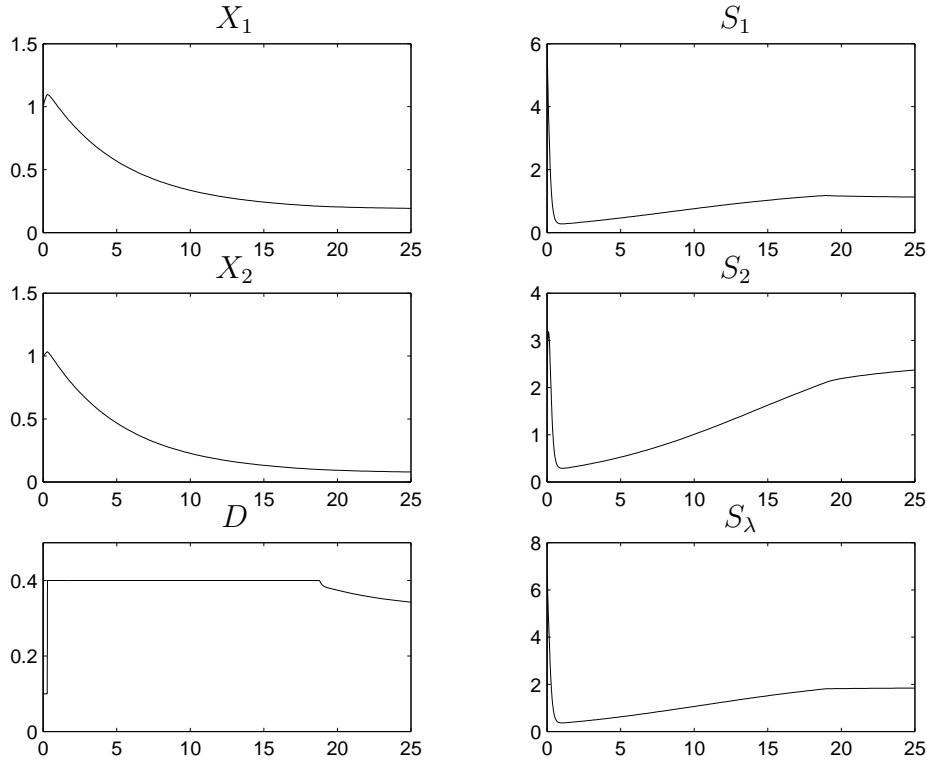


Figure 5: Time evolution of the states, control D , and output S_λ for the control system with the first set of initial conditions $(S_1, S_2, X_1, X_2)(0) = (6, 2, 1, 1)$

2.1.6 Conclusion

In this section, we have given a control law for the regulation of a model of anaerobic digestion with two bacteria. We have presented a control that regulates the pollution level: it ensures that the pollution level stays between a minimal and a maximal value while the dilution rate is also fixed between a minimal and a maximal value. No analysis of the actual behavior of the system inside the region where S_λ belongs to the desired interval has been made beyond the condition that we have given to ensure that the system has a single equilibrium, and the observation that there is no risk of wash-out of the bacteria inside that region.

Our controller requires that a measure of the pollution level is available online. If it is not the case, we will need to design an observer that will help reconstruct the value of S_λ from the available observations, namely the methane gaseous flow rate $= k_6 \mu_2(S_2) X_2$, and some measures of S_λ (made with large time intervals in between them). If the output of the observer is an interval, as in Section 2.1.4, we can apply the controller that we presented in that section. Our controller still needs to be implemented on the experimental setup.

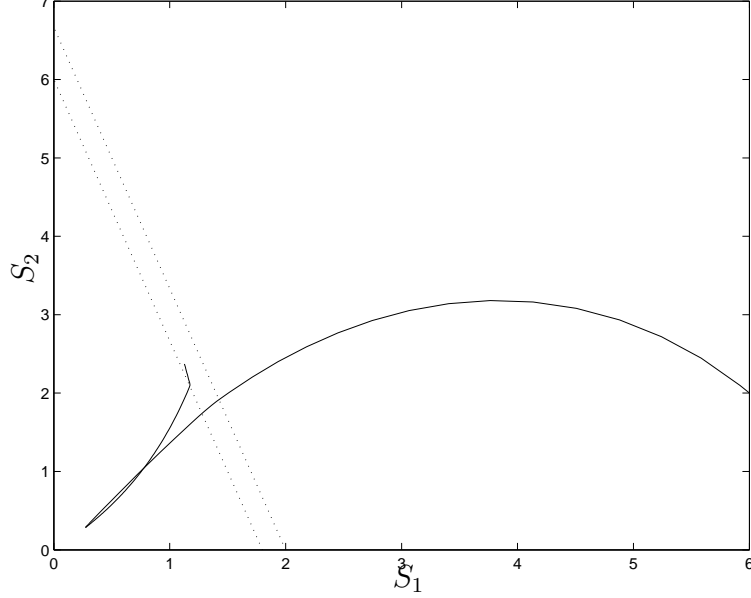


Figure 6: (S_1, S_2) phase plane for the control system with the first set of initial conditions $(S_1, S_2, X_1, X_2)(0) = (6, 2, 1, 1)$; the dotted lines represent the limits of region Ω_3

2.2 Static output feedback using methane flow rate measurements

The following section is the description of work that has been published in [19] and [20]. It tackles the problem of controlling the anaerobic digester with very few measurements (namely, only the methane flow-rate is measured online). As in the previous control method, this design is based on the analysis of the four dimensional AM1 model (1)

$$\begin{cases} \dot{X}_1 &= (\mu_1(S_1) - \alpha D)X_1 \\ \dot{X}_2 &= (\mu_2(S_2) - \alpha D)X_2 \\ \dot{S}_1 &= D(S_{1in} - S_1) - k_1\mu_1(S_1)X_1 \\ \dot{S}_2 &= D(S_{2in} - S_2) + k_2\mu_1(S_1)X_1 - k_3\mu_2(S_2)X_2 \end{cases}$$

In the considered process, methane solubility is very low, therefore the methane produced by the methanization step is not stored in the liquid phase. The output methane flow rate q_{CH_4} can then be written as a function of the state as follows:

$$q_{CH_4} = k_4\mu_2(S_2)X_2$$

The methane flow rate is measured online; let us denote this output $y = q_{CH_4} = k_4\mu_2(S_2)X_2$.

Usually, the most crucial problem in controlling equations (1) is the formulation of reasonable expressions for the corresponding specific growth rates: $\mu_1(S_1)$ and $\mu_2(S_2)$. It is therefore important to point out that the controller that we will develop does not assume any analytical expression for the growth rates (neither Monod, nor Haldane expressions are given). It is only supposed that the following assumption is satisfied:

Assumption 6 • μ_1 is a function of S_1 , $\mu_1(0) = 0$ and $\mu_1 > 0$ when $S_1 > 0$

- μ_2 is a function of S_2 , $\mu_2(0) = 0$ and $\mu_2 > 0$ when $S_2 > 0$

which ensures the positivity of the model (1) when $D(\cdot) \geq 0$.

2.2.1 Study of a simplified model of the anaerobic digestion

Simplified model presentation In this section we present a simplified model of the anaerobic digestion in order to introduce our controller. This model contains the main features that explain the destabilization by acid accumulation: the growth rate $\mu_2(S_2)$ is not monotonic and represents both the growth and the inhibition effect of acid accumulation. It can also be seen as a simplification of model (1) if $\mu_1(\cdot)$ is much larger than $\mu_2(\cdot)$ using the singular perturbation theory [17]. This two dimensional model has two locally stable equilibria. Note that the system is unstable because of the inhibition effect of acid accumulation.

$$\begin{cases} \dot{X}_2 = (\mu_2(S_2) - \alpha D)X_2 \\ \dot{S}_2 = D(S_{2in} - S_2) - k\mu_2(S_2)X_2 \end{cases} \quad (20)$$

The yield coefficient k represents the substrate degradation yield.

Asymptotic observer design In order to monitor the process, we propose here to build a software sensor that will estimate the VFA and the biomass in the digester on line, on the basis of the methane flow rate measurements.

Let us rewrite the model (20) using the measurement y :

$$\begin{cases} \dot{X}_2 = \frac{y}{k_4} - \alpha D X_2 \\ \dot{S}_2 = D(S_{2in} - S_2) - \frac{k}{k_4} y \end{cases} \quad (21)$$

We now propose the following simple estimates \hat{S}_2 and \hat{X}_2 for S_2 and X_2 , respectively:

$$\begin{cases} \dot{\hat{X}}_2 = \frac{y}{k_4} - \alpha D \hat{X}_2 \\ \dot{\hat{S}}_2 = D(S_{2in} - \hat{S}_2) - \frac{k}{k_4} y \end{cases} \quad (22)$$

Indeed, it is straightforward to see that the equation error

$$e = (e_1, e_2)^T = (X_2 - \hat{X}_2, S_2 - \hat{S}_2)^T$$

satisfies:

$$\dot{e} = (\alpha D(t)(\hat{X}_2 - X_2), D(t)(\hat{S}_2 - S_2))^T$$

and therefore:

$$\dot{e} = -D(t) \begin{pmatrix} \alpha & 0 \\ 0 & 1 \end{pmatrix} e$$

If $D(t)$ satisfies some good properties (e.g. $D(t) \geq D_{min} > 0$), then this proves that the error tends toward zero: the estimate converges.

This observer will be used in the practical implementation of the controller to monitor the VFA concentration and to check that the controller works properly. An important point is that the controller proposed in the sequel will not use the observer estimates.

The asymptotic controller design The objective of this section is to design a feedback that uses the measurement y to maintain the VFA concentration at a reference value \bar{S}_2 . More precisely, we choose the following dynamics for S_2 :

$$\dot{S}_2 = D(t)(\bar{S}_2 - S_2) \quad (23)$$

Note that, if $D(t) \geq D_{min} > 0$, this guarantees the convergence of S_2 toward \bar{S}_2 .

The chosen dynamics differ from the usual linearizing control [1] as it has been for example applied to anaerobic digestion [26, 7]. Indeed, here the dynamics can not be tuned (it is asymptotic). But, as we will see in the sequel, it leads to a more robust controller.

If we confront (23) with (21), this imposes:

$$D(t) = \frac{k}{k_4(S_{2in} - \bar{S}_2)}y \quad (24)$$

and our result follows:

Lemma 3 For any positive initial condition the control law (24) ensures that S_2 tends asymptotically toward \bar{S}_2 if $\bar{S}_2 < S_{2in}$.

Proof of Lemma 3: First let us take a small $\epsilon > 0$ such that $X_2(0) > \epsilon$ and $S_2(0) > \epsilon$. We first show that the following set:

$$I_\epsilon = \{(S_2, X_2), S_2 > \epsilon, X_2 > \epsilon\}$$

is positively invariant if ϵ is small enough. This is easily proven by considering the flow on the boundaries:

- For $X_2 = \epsilon$, and $S_2 \geq \epsilon$:

$$\dot{X}_2(X_2 = \epsilon) = \mu_2(S_2)\epsilon\left(1 - \frac{\alpha k \epsilon}{S_{2in} - \bar{S}_2}\right)$$

Let $\bar{X}_2 = \frac{S_{2in} - \bar{S}_2}{\alpha k}$, then, if $\epsilon < \bar{X}_2$, we have $\dot{X}_2 > 0$.

- For $S_2 = \epsilon$ and $X_2 > \epsilon$, we show in the same way that if $\epsilon < \bar{S}_2$ then $\dot{S}_2 > 0$. Finally, we choose: $0 < \epsilon < \min(\bar{S}_2, \bar{X}_2)$.

We have shown that $D(t) = \frac{k}{S_{2in} - \bar{S}_2}\mu_2(S_2)X_2 > 0$, consequently the observer (22) applied to the system (20) with the control law (24) converges towards the values of X_2 and S_2 .

Now let us consider the following Lyapunov function:

$$V_1(\xi) = \frac{1}{2}(\bar{S}_2 - S_2)^2 + \frac{1}{2}(\bar{X}_2 - X_2)^2$$

whose derivative is

$$\dot{V}_1(\xi) = -\frac{y}{k_4}\left(\frac{k}{S_{2in} - \bar{S}_2}(\bar{S}_2 - S_2)^2 + \frac{1}{\bar{X}_2}(\bar{X}_2 - X_2)^2\right)$$

Then $\dot{V}_1 \leq 0$ on the domain I_ϵ , and $\dot{V}_1 = 0$ only for (\bar{S}_2, \bar{X}_2) . It demonstrates the global asymptotic stability of the point (\bar{S}_2, \bar{X}_2) . ■

2.2.2 Study of the dimension 4 model

Control objectives Now we consider the dimension 4 model given by equations (1) and we want to choose and maintain constant the total amount of organic substrate in the fermenter. Let us denote $\tilde{S}_1 = \frac{k_1}{k_2} S_2$. It is the amount of COD needed (according to the yield coefficients) to obtain the quantity of VFA S_2 , after the biological degradation of \tilde{S}_1 by the acidogenic bacteria. So we introduce the variable S_T that is an equivalent of the total amount of organic substrate in the fermenter:

$$S_T = S_1 + \frac{k_1}{k_2} S_2$$

We then want to assign S_T to a chosen $\bar{S}_T < S_{Tin}$, where $S_{Tin} = S_{1in} + \frac{k_1}{k_2} S_{2in}$. \bar{S}_T is the acceptable level of pollution in the outflow of the bioreactor.

Now we rewrite system (1) using the new variable S_T , and injecting the output $y = q_{CH_4}$:

$$\begin{cases} \dot{X}_1 = (\mu_1(S_1) - \alpha D) X_1 \\ \dot{S}_1 = D(S_{1in} - S_1) - k_1 \mu_1(S_1) X_1 \\ \dot{X}_2 = \frac{y}{k_4} - \alpha D X_2 \\ \dot{S}_T = D(S_{Tin} - S_T) - \frac{k_3 k_1}{k_2 k_4} y \end{cases} \quad (25)$$

Observer design In the model (25), the equations for S_T and X_2 are the same as equations (21). Therefore the observer designed for the simplified model can be used without any modification to estimate X_2 and S_T . Remark that $S_1 \leq S_T$ and $S_2 \leq \frac{k_2}{k_1} S_T$. Thus, the estimate of the total COD in the digester provides us with an upper bound for S_1 and S_2 .

Controller design Let us look for $D(t) > 0$ ensuring, with a chosen \bar{S}_T :

$$\dot{S}_T = D(t)(\bar{S}_T - S_T) \quad (26)$$

it leads to

$$D(t) = \frac{k_3 k_1}{k_2 k_4 (S_{Tin} - \bar{S}_T)} y(t) \quad (27)$$

Notation 1 Let us define

- $\bar{X}_2 = \frac{k_2(S_{Tin} - \bar{S}_T)}{\alpha k_3 k_1}$, so that, with the control law (27), $\dot{X}_2 = \alpha D(t)(\bar{X}_2 - X_2)$.
- $\tilde{D}(S_1) = \frac{k_3 k_1}{k_2(S_{Tin} - \bar{S}_T)} \mu_2(\frac{k_2}{k_1}(\bar{S}_T - S_1)) \bar{X}_2$
for the considered value of S_{Tin} , \bar{S}_T and \bar{X}_2 . Note that $\tilde{D}(S_1)$ is $D(t)$ computed for $X_2 = \bar{X}_2$ and $S_T = \bar{S}_T$.
- $\tilde{\mu}_1(S_1) = \frac{\mu_1(S_1)}{\tilde{D}(S_1)}$.

Lemma 4 For any positive initial condition the control law (27) ensures that S_T tends asymptotically toward \bar{S}_T if $\bar{S}_T < S_{Tin}$.

Proof of Lemma 4: First we show that the model trajectories are bounded. For this we define the two following variables:

$$\begin{aligned} z_1 &= k_1 X_1 + S_1 \\ z_2 &= S_T + \frac{k_3 k_1}{k_2} X_2 \end{aligned}$$

Now it is straightforward that:

$$\begin{aligned} -D(z_1 - S_{1in}) &\leq \dot{z}_1 \leq -\alpha D(z_1 - S_{1in}) \\ -D(z_2 - S_{Tin}) &\leq \dot{z}_2 \leq -\alpha D(z_2 - S_{Tin}) \end{aligned}$$

proving that z_1 and z_2 are bounded; thus the state variables are bounded too.

Now we will use the boundedness of the state variables to show that X_2 and S_2 remain positive for any positive initial condition and therefore show that $D(t)$ remains positive. We will assume for the proof that the acidogenic growth rate is bigger than the methanogenic one, and therefore that a dilution rate that would not wash out the methanogenic bacteria would not wash out the acidogenic ones. Consequently, X_1 remains lower bounded by a positive number.

- We have easily $D(t) \geq 0$

$$\dot{X}_2(X_2 = \epsilon) = \alpha D(t)(\bar{X}_2 - \epsilon)$$

Then $X_2 \geq \min(\bar{X}_2, X_2(t_0)) > 0$. And:

$$D(t) = 0 \Leftrightarrow S_2 = 0$$

- Now we have to show that S_2 also remains positive for any positive initial condition.

We have assumed that $\exists \epsilon_1 > 0$, $X_1 > \epsilon_1$. Since $\dot{S}_T = D(t)(\bar{S}_T - S_T)$ and $D(t) \geq 0$, $S_T > 0$ for a positive initial condition. Since $S_T = S_1 + \frac{k_1}{k_2} S_2$, S_1 and S_2 can not cancel at the same time. For $S_2 = \epsilon_2 > 0$ small enough, $\exists \epsilon_3 > 0$, $S_1 > \epsilon_3$. And consequently, $\exists A > 0$, $k_2 \mu_1(S_1) X_1 > A$. Now we compute $\dot{S}_2(S_2 = \epsilon_2)$:

$$\dot{S}_2(S_2 = \epsilon_2) > A + B \mu_2(\epsilon_2) X_2$$

With $A > 0$. $B < 0$ if $\bar{S}_T < S_{1in}$. If we choose a good value for ϵ_2 and since X_2 is positive and bounded, we prove $\dot{S}_2(S_2 = \epsilon_2) > 0$ for any positive initial condition and so S_2 can not cancel.

We have shown that for any positive initial condition the state variables are bounded and remain positive, so $D(t)$ is bounded and remains positive too.

Note that $D(t)$ is also a function of the state variables and as $D(t) > 0$ we can make a time change $t_2 = \int_0^t D(\tau) d\tau$ (see *e.g.* [16]). The system (25) becomes:

$$\left\{ \begin{aligned} \frac{dX_1}{dt_2} &= \left(\frac{\mu_1(S_1)}{D(t)} - \alpha \right) X_1 \\ \frac{dS_1}{dt_2} &= (S_{1in} - S_1) - \frac{k_1 \mu_1(S_1)}{D(t)} X_1 \\ \frac{dX_2}{dt_2} &= \alpha (\bar{X}_2 - X_2) \\ \frac{dS_T}{dt_2} &= \bar{S}_T - S_T \end{aligned} \right. \quad (28)$$

The two last equations of (28) are decoupled from the two others and linear. It guarantees that for any positive initial condition X_2 and S_2 tends asymptotically to \bar{X}_2 and \bar{S}_2 . ■

Assumption 7 *We assume that:*

- $\bar{S}_T < S_{Tin}$
- for $S_1 \in [0, \bar{S}_T]$ the function $\mu_1(S_1)$ is increasing
- for $S_2 \in [0, \frac{k_2}{k_1}\bar{S}_T]$ the function $\mu_2(S_2)$ is increasing

This hypothesis is very reasonable: in practice we choose a low value for \bar{S}_T that will be under the inhibition threshold of μ_2 .

Lemma 5 Under Assumption 7 the point $\bar{\xi}$ of (1) with the controller (27) is globally asymptotically stable.

Proof of Lemma 5: Now let us consider the system (1) when X_2 and S_T have reached their equilibria. We have:

$$\begin{cases} \dot{X}_1 = (\mu_1(S_1) - \alpha \tilde{D}(S_1))X_1 \\ \dot{S}_1 = \tilde{D}(S_1)(S_{1in} - S_1) - k_1\mu_1(S_1)X_1 \end{cases} \quad (29)$$

Since $\tilde{D}(S_1) > 0$, we make the following change of time; we set $t_2 = \int_0^t \tilde{D}(S_1(\tau))d\tau > 0$, the system becomes then:

$$\begin{cases} \frac{dX_1}{dt_2} = (\tilde{\mu}_1(S_1) - \alpha)X_1 \\ \frac{dS_1}{dt_2} = (S_{1in} - S_1) - k_1\tilde{\mu}_1(S_1)X_1 \end{cases}$$

First, remember that we are on the surface given by $S_1 + \frac{k_1}{k_2}S_2 = \bar{S}_T$ and therefore $S_1 < \bar{S}_T$. Under Assumption 7, the application μ_1 is increasing on the interval $S_1 \in [0, \bar{S}_T[$ and $\mu_2(\frac{k_2}{k_1}(\bar{S}_T - S_1))$ is decreasing. Finally, on this interval, $\tilde{\mu}_1$ is an increasing application such that $\tilde{\mu}_1(0) = 0$. This corresponds to the classical chemostat equation, whose behavior is simple [29]: it has a single globally stable equilibrium. ■

Note that the demonstration is not based on any analytical formulation of the growth rates μ_1 and μ_2 , that is particularly important for the robustness of the controller.

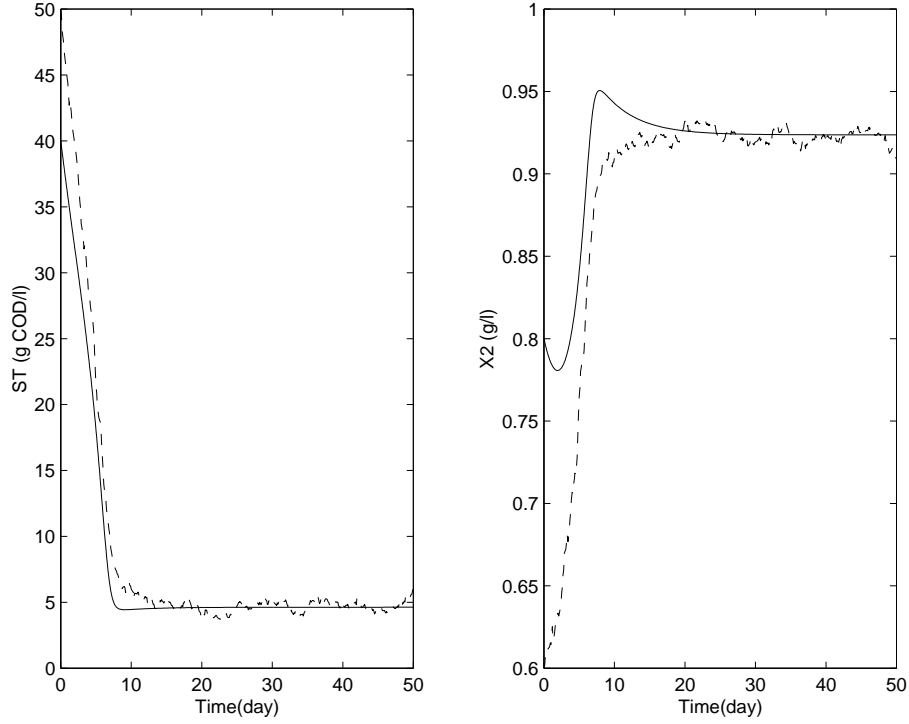


Figure 7: Simulation of the observer for S_T and X_2 with a 40% noise on the output y .

2.2.3 Simulation study

In this section, the parameter values given by [3] have been chosen to run the model. A multiplicative white noise η of variance 0.4 has been added to the measurement of the methane flow rate generating a 40% proportional noise:

$$y = q_{CH_4}(1 + \eta)$$

$\bar{S}_T = 2gCOD/L$ is chosen as the desired set point of S_T . With the kinetics expression of [3] (μ_1 and μ_2 are of the Monod and Haldane type, respectively), Assumption 7 is fulfilled, and therefore the hypotheses of Lemma 5 are satisfied. Then it is straightforward that the results will agree with our predictions: the plant is prevented from biomass washout and has a single GAS equilibrium for a fixed set of parameters.

The results of the observer are plotted on Figure 7. Note that the measurement noise is filtered, and the quality of the estimates is good.

The controller results can be seen on Figure 8. Despite the high level of noise the controller action is efficient and the total COD remains in a reasonable interval. The converging rate is fast and the controller is robust towards variations of the influent COD concentration.

Moreover, in order to take into account the fact that the influent pollutant concentration can change as time goes on during the process operation, a piecewise constant $S_{T_{in}}$ is imposed during the simulation. It is important to note that, in order to maintain S_T at its equilibrium, $S_{T_{in}}$ variations have to be known and actualized in the feedback gain (see control law (27)).

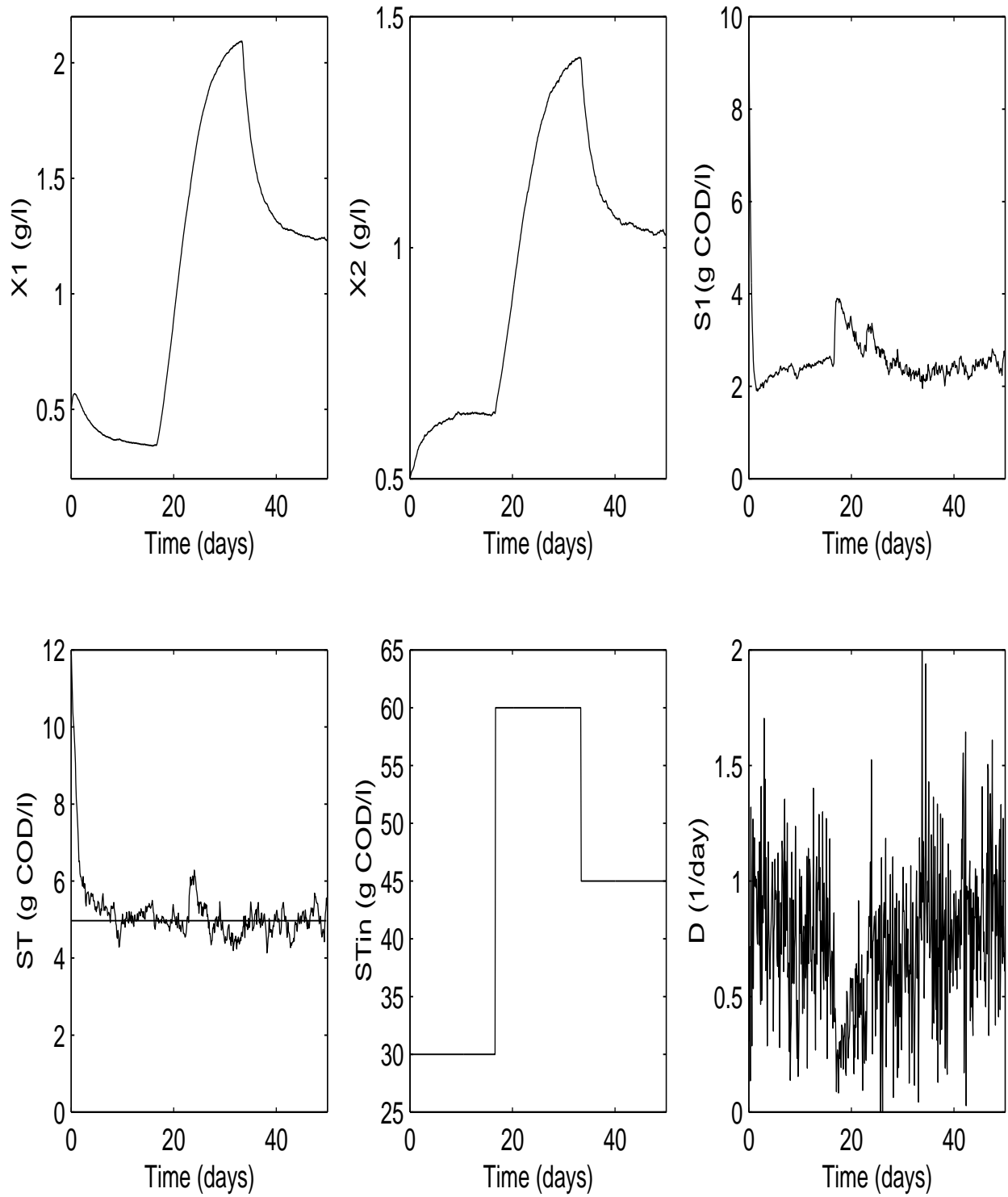


Figure 8: Simulation of the controller with variations of the influent COD charge and with a 40% noise on the output y .

However, it appears that despite these variations in the influent and the high level of noise on the output, the variable S_T remains in a very small interval around its chosen equilibrium value $\bar{S}_T = 2gCOD/L$. From equation (26), one can notice that the converging rate of the closed loop system is non-linear and not adjustable by an operator. In spite of this drawback, the converging rate seems to be fast enough for wastewater treatment.

2.2.4 Experimental results

To validate this mathematical approach of the control of anaerobic digestion processes, real-life experiments were also performed under various operating conditions with the following experimental set-up:

The influent. The experiments were performed with raw industrial wine distillery vinasses obtained from local wineries in the area of Narbonne, France. This substrate, neither sterile nor homogeneous, is stored in three $27 m^3$ tanks connected to the reactor by a piping system of about $0.5 m^3$. The main characteristics of the influent are given in the following table

Component	Range
VFA (g/l)	[5-6]
Total COD	[9-17.4]
Alkalinity (meq/l)	[30.8-62.4]
pH	[5-5.4]

The process is an up-flow anaerobic fixed bed reactor made of a circular column of $3.5m$ height, $0.6m$ diameter and a useful volume of $0.948m^3$. The reactor is highly instrumented with the following measurements available on-line every 2 minutes: input and recirculation liquid flow rates, pH of the reactor and of the input wastewater, heater and reactor temperatures, biogas output flow rate, CO_2 , CH_4 and H_2 composition in the gas phase and total organic carbon (TOC) in the reactor. Other measurements are available every half hour using a titrimetric sensor [5] and a mid infra-red spectrometer [31] : total volatile fatty acids (VFA), soluble chemical oxygen demand (COD), bicarbonate concentrations and total and partial alkalinity in the liquid phase. More details about the process and evaluation of its on-line instrumentation are available in [30].

For clarity, these experiments are introduced in two different parts: first, the usual operating conditions for wastewater treatment (i.e., no failures in the equipment); then since some breakdowns occurred as the experiments were carried out, the safe behavior of the controlled plant is shown. Note that this situation could have been hazardous for the reactor without any regulation procedure.

Normal operating conditions. In these operating conditions, the reactor follows model (1). Thus, the controlled plant is expected to have the simple behavior the control law has been designed for. In particular, the pollutant concentration S_T must follow the non-linear equation (26) but since this equation is non-linear, it is difficult to ensure that S_T has the good quantitative behavior. However, it can be noticed that S_T has to follow the same qualitative behavior that equation (26) predicts: S_T should follow a first order behavior with a variable positive gain. In other words, if S_T is below (respectively above) its chosen set point, it will increase (respectively decrease) exponentially (but not at a constant speed) towards its chosen set point.

Two transient behaviors for the input variable D and for the controlled variable S_T are illustrated in Figure 9. The other variables are not represented since the key points of the control action

are presented with these two. It is worth noting that the controller action is efficient and agrees with our mathematical predictions: S_T qualitative behavior is as expected to be. Moreover, despite the fact that the convergence rate is not adjustable, it seems to be fast enough for wastewater treatment.

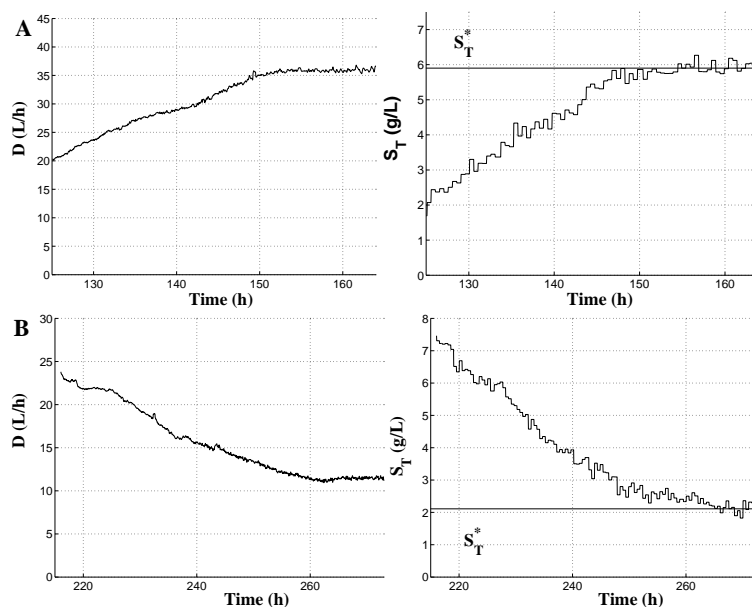


Figure 9: Evolution of the controlled process. The dilution rate D and the value of S_T are represented for two experiments (A and B) on the up-flow anaerobic fixed bed digester

Breakdown operating conditions. As usual in real-life experiments, some unforeseen failures happened on the reactor devices. Therefore, the process model differs from model (1) or, at least, the controlled plant behavior differs from its expected dynamical behavior. It is worth noting that most of plant breakdowns occur together with a decrease in the output biogas (methane) flow rate (so does the output y). What is interesting in the present regulation procedure is that, for the closed loop plant, a decrease in the output y will lead to reducing the dilution rate. This is indeed the easiest way to prevent the reactor from biomass washout, that could have happened because of the process failure.

This phenomenon is highlighted on Figure 10. In this experiment, a problem in the mixing between influent vinasses and water in the dilution system has occurred. Then, the digester has been fed with pure water. If the process was run in open loop, the biomass would have quickly decreased and been washed out of the reactor. For the controlled system, since the methane flow rate decreases, the dilution rate decreases too, leading D to its minimal value (i.e., 5 L/h, imposed by the process configuration). This prevents on one hand the biomass from short-term washout and, on the other hand, provides the required time to human operators to fix the problem.

2.2.5 Conclusion

A robust non-linear controller has been proposed for a fixed bed anaerobic digestion pilot process and we have proven its convergence for a mass-balance model independently from the model's

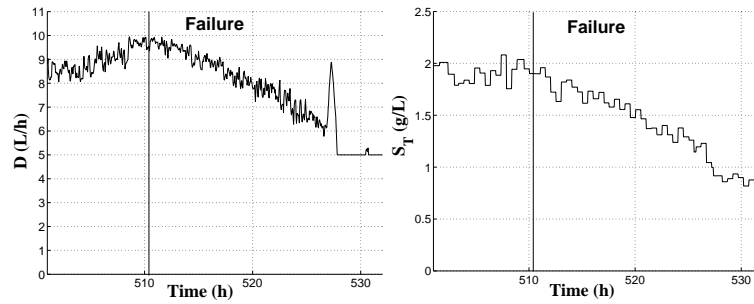


Figure 10: Evolution of the process in closed loop during a plant failure (the digester has been fed with pure water)

biological uncertainty. This controller is very simple in its design since it only consists in an output feedback law. The single required parameter is the feedback gain that can be tuned online (i.e., by trials and errors) by moving this gain to reach the desired set point value for S_T . A simulation study has shown that this regulation procedure is very robust to high level of noise and insensitive to variations of the influent pollutant concentration. To validate our approach in real life, regulation experiments were performed on the pilot digester. The closed loop plant experimental results agreed with our theoretical predictions and exhibited an unexpected but interesting safe behavior towards some hazardous plant failures.

It is worth noting that this regulation procedure can also be applied to the model presented by [4]. This dimension 6 model is an extension of model (1) with two other equations in cascade; one for alkalinity and the other for the total dissolved inorganic carbon. Therefore the control law will globally stabilize the more general dimension 6 model as well.

Another point which is important to emphasize is that this controller regulates the value of a variable (related to the COD) which is not measured on line. As a consequence, with this control approach, it is not mandatory to have an on-line sensor for the COD measurements, which is often a limiting step for the implementation of a controller. It also explains why this type of controller cannot be compared e.g. to a PID which would require on-line COD measurements. Nevertheless, to avoid drifts, some off-line values of the COD are required to regularly recalibrate the controller. Therefore, an adaptive version of the control law (27), based on off-line values, is presented in the next section. This method ensures an automatic controller tuning without model identification.

2.3 Adaptive output feedback using methane flow rate measurements

A direct extension of the controller that was presented in the previous section consists in adapting the parameter that multiplies y in the feedback control law (27). Indeed, in the preceding controller, an exact knowledge of the model parameters was necessary in order to achieve the regulation of the COD at a prespecified value. In this section, this exact regulation is achieved through an automated tuning of the parameter of the control law. The following section is the description of work that is accepted for publication ([21]).

2.3.1 Study of a simplified model of the anaerobic digestion

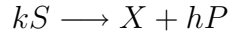
The control design and stability analysis was, in this case, not performed on model (1); it was instead done on a model that represents the whole process with two states: the total biomass X_T and the total COD S_T . In this simplification of the model, the specific growth-rate is often taken to be of the Haldane type:

$$\begin{cases} \dot{X}_T &= (\mu_T(S_T) - \alpha D)X_T \\ \dot{S}_T &= D(S_{Tin} - S_T) - k_3\mu_T(S_T)X_T \end{cases} \quad (30)$$

In fact, the control design was achieved with the following model

$$\begin{cases} \dot{X} &= r(S, X) - \alpha DX \\ \dot{S} &= D(S_{in} - S) - kr(S, X) \\ \dot{P} &= hr(S, X) - \beta DP \end{cases} \quad (31)$$

where P is concentration of the product of the reaction



in the liquid phase. Our process takes this form with $S = S_T$, $X = X_T$ and $P = CH_4$. However, as we stated in the previous section, the methane solubility is very low, so that the produced methane is mainly gaseous. The dissolved methane then remains at steady state and of zero concentration, so that the P part of the model does not need to be considered, and we can concentrate on (30) instead of (31).

It has been shown, in the previous section, that the application of the controller

$$D = \frac{k_3}{k_4(S_{Tin} - \bar{S}_T)} q_{CH_4} = \frac{k_3}{k_4(S_{Tin} - \bar{S}_T)} k_4 \mu(S_T) X_T$$

yielded regulation of the equilibrium (\bar{X}_T, \bar{S}_T) corresponding to the COD value $S_T = \bar{S}_T$, as long as the parameters k_3 and k_4 were exactly known. It is now suggested to replace the $\frac{k_3}{k_4(S_{Tin} - \bar{S}_T)}$ by a parameter γ in the control law; this γ will be adapted, so that the required regulation of $S_T = \bar{S}_T$ is achieved. It is now assumed that

Assumption 8 *Suppose that*

- μ_T is a C^1 function such that $\mu_T(S_T) > 0$ when $S_T > 0$,
- $\bar{S}_T < S_{Tin}$
- *the following quantities are measured online:*

$$\begin{cases} y_1 &= k_4 \mu_T(S_T) X_T \\ y_2 &= S_T \end{cases}$$

Real sensors or numerical estimators [9] can indeed be used to obtain online the quantity y_1 . In practice, the substrate S_T is often not available online, but low frequency measurements are available (for pollution control). The philosophy of our controller is based on this statement, and the adaptation of the unknown parameters will be performed at the low rate imposed by the substrate measurements. Of course, if hard or soft measurements of S_T were available online, results would be better and convergence faster. Remark that, for a large part of bioprocesses beyond anaerobic digestion, the production (or consumption) of gaseous components ($O_2, CO_2...$) is monitored and is directly related to the reaction kinetics, therefore to some function in the form of y_1 [20].

Let us denote $\chi = (X_T, S_T, \gamma)$ the new state vector and $\bar{\gamma} = k_3/(k_4(S_{Tin} - \bar{S}_T))$.

Proposition 1 *Under Assumption 8, the nonlinear adaptive feedback control law:*

$$\begin{cases} D(.) = \gamma(t)y_1 = \gamma(t)k_4\mu_T(S_T)X_T \\ \dot{\gamma} = Ky_1(\bar{S}_T - y_2)(\gamma - \gamma_m)(\gamma_M - \gamma) \end{cases} \quad (32)$$

With: $0 < \frac{k_3}{k_4 S_{Tin}} < \gamma_m < \gamma^* < \gamma_M$ and $K > 0$

globally stabilizes system (1) towards the positive set point $\bar{\chi} = (\bar{X}_T, \bar{S}_T, \bar{\gamma})$.

Proof: The control law (32) yields the closed loop system:

$$\begin{cases} \dot{X}_T = y_1(\frac{1}{k_4} - \alpha\gamma X_T) \\ \dot{S}_T = y_1[\gamma(S_{Tin} - S_T) - \frac{k_3}{k_4}] \\ \dot{\gamma} = Ky_1(\bar{S}_T - y_2)(\gamma - \gamma_m)(\gamma_M - \gamma) \end{cases} \quad (33)$$

In the sequel we will only consider positive initial conditions $X_T(0)$, $S_T(0)$, and $\gamma(0)$ such that $\gamma(0) \in (\gamma_m, \gamma_M)$. With these initial conditions X_T , S_T remain non-negative and γ remains in (γ_m, γ_M) . Using γ boundary values, we show that $\forall t \geq 0$ the state variables $S_T(t)$ and $X_T(t)$ remain positive; thus using the positiveness of μ_T for $S_T > 0$, we conclude that $y_1 = \mu_T(S_T)X_T$ is bounded below by a positive constant. We are now able to make the time change $t' = \int_0^t y_1(\tau)d\tau$ [6] and the change of coordinates: $(v, x) = (S_{Tin} - S_T, X_T)$. The closed loop system (33) becomes (denoting with a prime the time derivatives with respect to t' , and $\bar{v} = S_{Tin} - \bar{S}_T$):

$$\begin{cases} x' = (\frac{1}{k_4} - \alpha\gamma x) \\ v' = \bar{\gamma}\bar{v} - \gamma v \\ \gamma' = K(v - \bar{v})(\gamma - \gamma_m)(\gamma_M - \gamma) \end{cases} \quad (34)$$

The dynamical system (34) is an autonomous triangular system [32]: the system in v and γ does not depend upon the other variable x . Now we consider the sub-system in v and γ :

$$\begin{cases} v' = \bar{\gamma}\bar{v} - \gamma v \\ \gamma' = K(v - \bar{v})(\gamma - \gamma_m)(\gamma_M - \gamma) \end{cases} \quad (35)$$

First we want to show that the state of system (35) enters the set $\{v > 0\}$ in finite time. Considering the dynamics of $v(t)$ in the set $v \leq 0$, we show that $v' \geq \bar{\gamma}\bar{v} > 0$, which proves that v enters the set $\{v > 0\}$ in finite time. In the sequel, we will consider the initial time (by time translation if necessary) belonging to the set $\mathcal{E} = \{v > 0, \gamma \in (\gamma_m, \gamma_M)\}$.

We introduce the Lasalle function used by [13] in the context of Lyapunov stability for predator-prey models:

$$W(v, \gamma) = \int_{\bar{v}}^v \frac{w - \bar{v}}{w} dw + \int_{\bar{\gamma}}^{\gamma} \frac{w - \bar{\gamma}}{K(w - \gamma_m)(\gamma_M - w)} dw$$

We check that $W(v, \gamma)$ is defined, non-negative on \mathcal{E} and vanishes only for $v = \bar{v}$ and $\gamma = \bar{\gamma}$. Furthermore:

$$W' = - \left(\frac{\bar{\gamma}}{v} (\bar{v} - v)^2 \right)$$

Thus, W' is defined and negative on \mathcal{E} and vanishes only for $v = \bar{v}$. Lasalle's theorem implies that every solution of system (35) approaches the largest invariant set in the domain defined by $W' = 0$ [17]; let us denote this set $\Omega = \{v = \bar{v}, \gamma \in (\gamma_m, \gamma_M)\}$. Now, consider a trajectory initialized in Ω at $v = \bar{v}$ and $\gamma \neq \bar{\gamma}$; with respect to system (35) it is clear that this trajectory escapes from Ω and therefore that the largest invariant set in Ω is the fixed point $(\bar{v}, \bar{\gamma})$. Then $(\bar{v}, \bar{\gamma})$ is a globally attractive fixed point for system (35).

Straightforward Jacobian matrix computation at the point $(\bar{v}, \bar{\gamma})$ proves that this fixed point is locally stable too. Then, we conclude that $(\bar{v}, \bar{\gamma})$ is a globally asymptotically stable (GAS) fixed point for system (35).

Now let us study the behavior of the last state variable x on the set defined by $v = \bar{v}$ and $\gamma = \bar{\gamma}$. We have:

$$x' = \frac{1}{k_4} - \alpha \bar{\gamma} x$$

The corresponding system is linear and has a single equilibrium in $\bar{x} = \frac{1}{k_4 \alpha \bar{\gamma}}$ which is GAS. In order to finish the proof, we need the following result for autonomous triangular systems, which is proved in [32].

Lemma 6 Consider the triangular system in \mathbb{R}^n :

$$(\Sigma) \begin{cases} \dot{z} = f(z, w) \\ \dot{w} = g(w) \end{cases}$$

with: $z \in \mathbb{R}^{n-k}$, $w \in \mathbb{R}^k$, $f(\cdot)$ and $g(\cdot)$ \mathcal{C}^1 functions. Moreover we assume that:

A1: $w = 0$ is a GAS fixed point for $\dot{w} = g(w)$

A2: $z = 0$ is a GAS fixed point for $\dot{z} = f(z, 0)$

A3: every forward orbit of system (Σ) is bounded

Then, 0 is a GAS fixed point for system (Σ)

Note that assumptions (A1) to (A3) hold for system (34). Thus applying the Lemma (after state translation) to system (34), we conclude that the fixed point defined by $v = \bar{v}$, $\gamma = \bar{\gamma}$, and $x = \bar{x}$ is a GAS fixed point for (34). Thus, coming back to the original time and state variables, we conclude that the control law (32) globally stabilizes system (1) towards the point \bar{x} . ■

Remark 2 *If we want to regulate X_T , we can build an adaptive control using X_T measurements with a set point \bar{X}_T . For example for X_T we have:*

$$\dot{\gamma} = K(X_T - \bar{X}_T)(\gamma_m - \gamma)(\gamma_M - \gamma)$$

with: $0 < \frac{k_3}{k_4 S_{Tin}} < \gamma_m < \frac{1}{k_4 \alpha X_T} < \gamma_M$

Remark 3 Suppose kinetics measurement is corrupted by a (small) relative perturbation $\eta(t)$ such that $y_1 = (1 + \eta)\mu_T(S_T)X_T$. Then, since y_1 is in factor in system (33), one can show that the state remains asymptotically in a ball centered on $\bar{\chi}$ (with a radius proportional to η), highlighting the controller's robustness.

2.3.2 The problem of discrete time y_2 measurements

In practice the substrate S_T is sometimes only available at low frequency time measurements $y_2(iT) = S_T(iT)$ (T the sampling period). We show that the control law (32) still works, but requires slow adaptation, *i.e.* a small K .

Indeed, we can choose a K small enough ensuring that γ is a slow variable of the closed loop system while S_T and X_T are fast ones. Singular perturbation theory [17] applies, such that S_T remains on the manifold $S_T = S_{Tin} - k_3/k_4\gamma$. Straightforward calculus shows that the adaptive equation is such that $\forall t \in [iT, (i+1)T)$:

$$\dot{\gamma} = y_1 \frac{K k_3}{k_4 \bar{\gamma} \gamma(iT)} (\bar{\gamma} - \gamma(iT)) (\gamma - \gamma_m) (\gamma_M - \gamma)$$

Integrating this equation between iT and $(i+1)T$, we find the recurrent expression of $\gamma((i+1)T)$. Then, we show that a sufficient condition for the convergence of the sequence $(\gamma(iT))_{i \in \mathbb{N}}$ towards $\bar{\gamma}$ is:

$$0 < T < \frac{1}{K} \left[\frac{2k_4 \bar{\gamma} \gamma_m}{k_3 \max(y_1) (\gamma_M - \gamma_m)^2} \right]$$

Then for all sampling period T , there exists a small enough K , such that T fulfills this necessary condition.

2.3.3 Simulations

The anaerobic digestion model that has been used for simulation uses an Haldane function for the specific growth rate:

$$\mu_T(S_T) = \frac{\mu_m S_T}{K_m + S_T + S_T^2/K_i}$$

The model is simulated to evaluate the benefits of the control law (32) through comparison between open loop and closed loop performances. Together with a substrate concentration set point $\bar{S}_T = 4$ gCOD/L, we assume the following realistic parameters' values $\alpha = 0.8$, $\mu_m = 0.9$ day⁻¹, $K_m = 9$ g/L, $K_i = 3$ g/L, $k_3 = 2$, $\gamma_m = 0.1334$ L/g, $\gamma_M = 0.4$ L/g and $K = 0.8$.

Results are shown in Figure 11. For the open loop model, it results in applying the dilution $\bar{D} = \mu(\bar{S}_T)/\alpha = 0.2455$ day⁻¹ (note that the model parameters' values are required to compute \bar{D}), while for the closed loop model, the control law is computed from the expression (32), and the continuous measurements y_1 and y_2 . We choose a piecewise constant influent pollutant concentration S_{Tin} (unknown) to highlight the adaptive controller's action.

In addition to very smooth control actions (see the dilution rate in Figure 11) and a very good regulation of the substrate concentration (see Figure 11), the control law is able to estimate the influent concentration (from the other parameters knowledge) which is very interesting in practical applications (S_{Tin} is indeed very difficult to measure in practice).

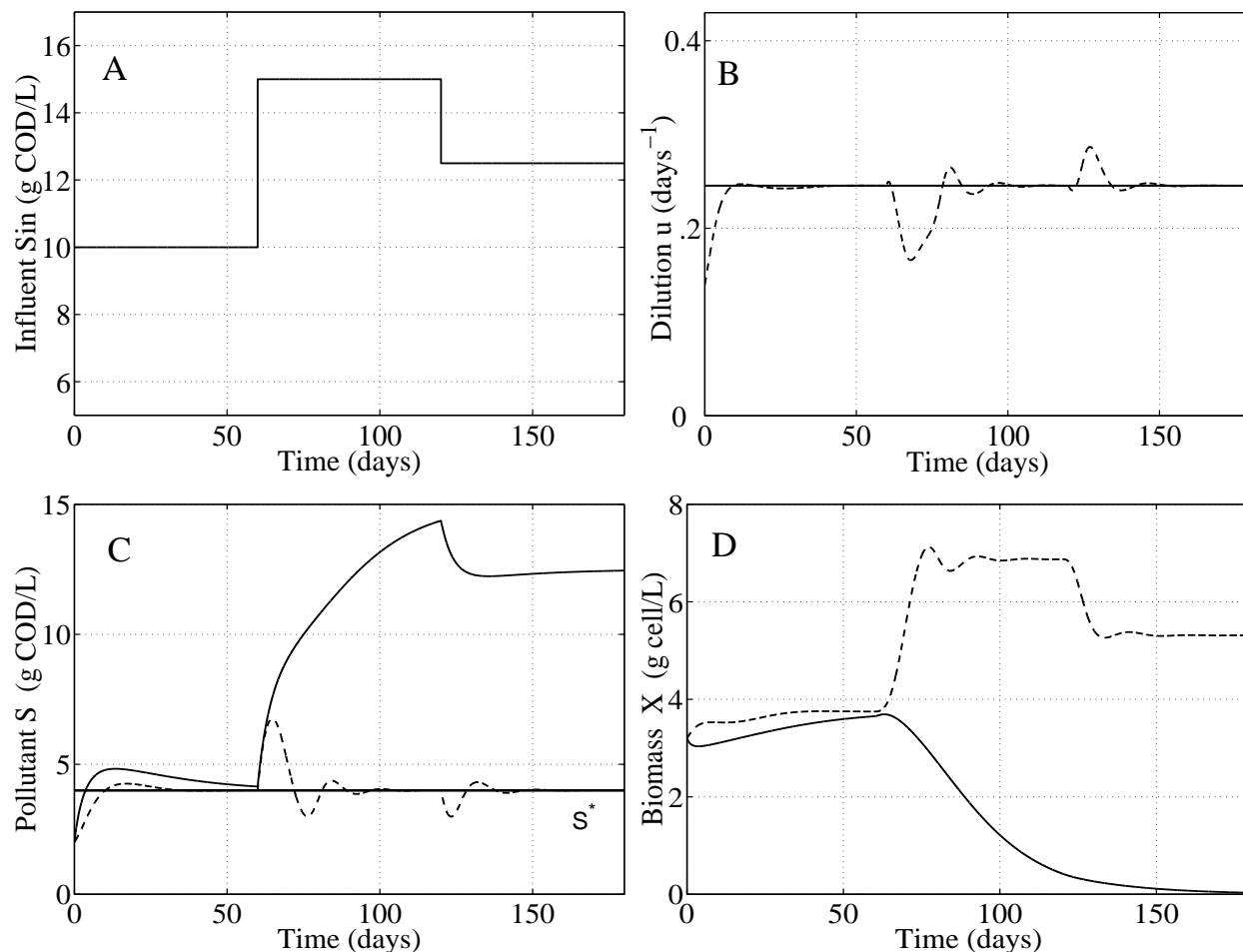


Figure 11: Simulations of the open loop plant (continuous line) and of the closed loop plant with the control law (32) (dashed line) (figures B, C, D). On figure A the piecewise constant influent concentration S_{Tin} (continuous line) is shown. Note that the step in S_{Tin} is lethal for the open loop digester.

It must be kept in mind that the destabilization (see *e.g.* the open loop system in Figure 11) of the process implies the disappearance of the biomass from the digester. Then the digester has to be inoculated again, which is a process that can last for months. During this operation, wastewater is no more treated.

From $t = 0$ to $t = 60$ both the open loop and the closed loop systems converge towards the equilibrium corresponding to the set point $S_T = \bar{S}_T$. At $t = 60$, influent substrate concentration increases from 10 to 15gCOD/L. On the one hand, it results in the destabilization of the open loop process: the biomass starts to be washed out of the bioreactor. On the other hand, the closed loop process escapes from the equilibrium $S_T = \bar{S}_T$ for a short time, but the control law (32) drives the

state variables back towards the equilibrium corresponding to the set point $S_T = \bar{S}_T$; the change of S_{Tin} has been efficiently rejected. Then, at $t = 120$, S_{Tin} decreases from 15 to 12.5gCOD/L. Destabilization of the open loop system still goes on despite the decrease of S_{Tin} . The control law remains efficient and rejects the s_{in} change again.

Remark 4 *It is important to notice that despite the (only) daily measurements of substrate concentration the control action remains efficient, but of course the convergence rate could be faster with online measurements of substrate concentration.*

2.3.4 Virtual plant

No real life experiment of the adaptive controller has been carried out yet, but an accurate virtual plant has been developed, based on the IWA Anaerobic Digestion Model No.1 (ADM1, [2]). This ADM1 model turns out to be the most accurate in its representation of the anaerobic process. However, its complicated structure makes it very hard to handle from a mathematical point of view. Though it is too complex to serve directly as a base for a controller, it can be used within a virtual plant to check the behavior of the controller in a validated realistic context. We have proven in this section, and shown in the simulations part, that our controller was very efficient for the 2-dimensional model of anaerobic digestion, upon which it was developed. In this section we will show that it is up to the task when faced with a more realistic model of the anaerobic digestion process.

The model ADM1 has been implemented using Simulink ([33]); the parameters that have been used are the default parameters from ADM1, with the exception of the solid retention time that we have calibrated on the basis of data obtained during an acidification phase because it is very sensitive. Three versions of the controller have been tested: the simple proportional controller, assuming a known value of the influent COD_{in} ; an adaptive controller, without knowledge of the influent concentration and an adaptive controller assuming a known value of the influent COD_{in} .

As an example, Figure 12 shows the results obtained for the simple non-adaptive controller coupled with the virtual plant where the influent COD concentration starts at 10 gCOD/L, at time 4 increases up to 20 gCOD/L, at time 8 increases again up to 25gCOD/L and finally at time 11 is restored to 10 gCOD/L. The set point value \bar{S}_T is fixed to 0.31 gCOD/L and the γ value used is 2.752. Though COD regulation is not precise, it remains in an admissible small set around COD despite the high influent concentrations changes.

The simulation results obtained for the proposed controllers applied to the model ADM1 are good and validate our approach. The first controller turns out to be the more sensitive to changes in the influent so that a little bias in the COD might be observed. The second one reacts less rapidly but is able to track a change in the influent. The last controller is the more accurate and presents the fastest convergence rate and the best robustness properties.

2.3.5 Conclusion

An adaptive version of the controller that was presented in Section 2.2 has been proposed. The global asymptotic stability of the regulated plant towards a chosen operating point has been proven, with the laws fulfilling the input non-negativity constraint. Originally, no assumption was made about the analytical expression of the bioreaction's kinetics $r(\cdot)$ (though, in this report, we have

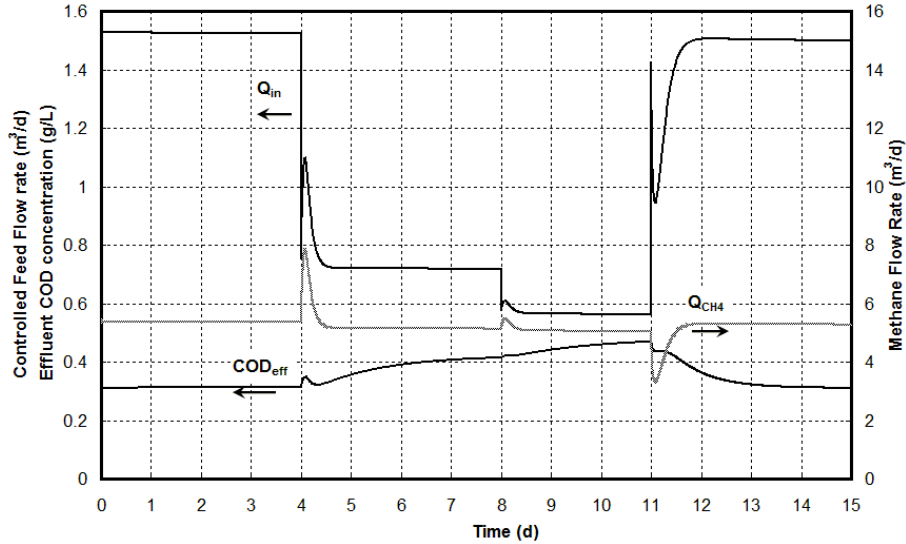


Figure 12: Application of the controller (27) to the virtual plant

limited our presentation to the case $r(\cdot) = \mu(S)X$. In addition, these control laws are robust to a relative noise on $r(\cdot)$ measurements and the adaptive law does not require any model parameters.

Some other work shows that the simple controller (27) can also be applied to other bioreaction schemes such as variable yield bioreactions [22] or “cascade” bioreactions [20]. More work is required for extended generalization.

Finally, the application of our controller to a virtual plant based on the ADM1 model show the practical relevance of our approach.

2.4 Simultaneous regulation of the substrate and the VFA

In this section we show a simple approach to regulate the two more important variables in anaerobic digestion: the organic load concentration and the volatile fatty acids concentration. We show how this approach is robust against uncertainties about input concentrations, kinetics parameters and yield coefficients that can be expressed as guaranteed intervals. In comparison with previous works, the control objective is not here to regulate these variables around a precise set-point but to lead them to a guaranteed control zone. This can be seen as an advantage if we only require that the regulated variable(s) does/do not surpass some limits but it is allowed to evolve inside them. As a consequence, fewer conditions are required and we use a more flexible control law.

In this work, we present two cases. The first one is the regulation of the organic load concentration S_1 and the second one is the simultaneous regulation of S_1 and the volatile fatty acids concentration S_2 . This work is based on the analysis of the model (1).

2.4.1 The regulation of S_1

In order to show the basic idea of this approach we show in this section the regulation of S_1 using the dilution rate D as the control variable. The control objective is to lead and to maintain S_1 inside

a pipe delimited by the interval $S_{1min} < S_1 < S_{1max}$. Several reasons can justify this choice. Here after we draw some of them.

a) From an ecological point of view, we want to guarantee the respect of the ecological norms. At this regard, all concentration staying below the maximum limit S_{1max} is suitable.

b) From a performance point of view, leading S_1 to a very low concentration would implicate very large retention times. This may be a disadvantage when the feed rates of wastewater entering the plant increase. We then have an interest in maintaining S_1 above a minimum S_{1min} .

c) From an operational point of view, a control law allowing S_1 to evolve inside a pipe may be more flexible and thus, less stressing than setting a fixed set-point.

d) From a more general control point of view, the regulation of S_1 might not be the only control objective: we might have an interest in other control objectives. These objectives can probably also be achieved if enough control freedom remains after the regulation of S_1 ; this freedom is characterized by the interval.

In this first part, we will drastically simplify model (1). In order to do that, we make the following assumption, which is often satisfied if the plant remains in a reasonable region of operation:

Assumption 9 *The concentration of acidogenic bacteria is not measured but it is quasi-constant: there exists $K > 0$ such that $K \approx k_1 X_1(t)$ for all $t \geq 0$.*

Given that the objective is the regulation of S_1 , and under Assumption 9, the only remaining relevant dynamics are the S_1 dynamics, which become:

$$\dot{S}_1 = D(S_{1in} - S_1) - K\mu_1(S_1) \quad (36)$$

Additionally we consider that S_1 is measured on-line. Let us now consider the two following stable equations

$$\begin{aligned} \dot{S}_1 &= D(S_{1max} - S_1) \\ \text{and } \dot{S}_1 &= D(S_{1min} - S_1) \end{aligned} \quad (37)$$

where S_{1max} and S_{1min} are constants with $S_{1min} < S_{1max}$. Then, the basic idea is to find a control law D such that the closed loop dynamics of S_1 is involved between these two stable trajectories, that is:

$$D(S_{1min} - S_1) \leq D(S_{1in} - S_1) - K\mu_1(S_1) \leq D(S_{1max} - S_1) \quad (38)$$

Assuming that $S_{1max} \leq S_{1in}$, it is clear from (38) that D must satisfy the following inequality:

$$\frac{K\mu_1(S_1)}{S_{1in} - S_{1min}} \leq D \leq \frac{K\mu_1(S_1)}{S_{1in} - S_{1max}} \quad (39)$$

Any $D(t)$ that satisfies this constraint will yield satisfaction of the control objective. In the particular case where $S_{1min} = S_{1max}$, D is uniquely defined by (39) and results in a controller that is highly similar to the one that was presented in Section 2.2.

In (39) the knowledge of all the terms on the extremes of the inequality is necessary. However, the knowledge on kinetics parameters, yield coefficients and process inputs is weak. We then formally introduce uncertainties as follows:

Assumption 10 The parameters S_{1in} , K , μ_{1max} and K_{S_1} are unknown, but there exist some known and strictly positive quantities (possibly time-varying) K_{max} , K_{min} , $S_{1in,min}$, $S_{1in,max}$, and functions $\mu_{1min}(S_1)$ and $\mu_{1max}(S_1)$ such that:

- a) $K_{min} \leq K \leq K_{max}$
- b) $\mu_{1min}(S_1) \leq \mu_1(S_1) \leq \mu_{1max}(S_1)$
- c) $S_{1in,min} \leq S_{1in} \leq S_{1in,max}$

In spite of these uncertainties it is possible to get that S_1 is stabilized in the inner neighborhood zone delimited by the control pipe $[S_{1min}, S_{1max}]$. Furthermore, the stability given by (39) can still be partially used. In addition, we are interested to using a strictly positive control law. These ideas are formally stated in the following proposition:

Proposition 2 Let Assumptions 9 and 10 be satisfied then, for any $S_{1in,min} > S_{1max} > S_{1min} > 0$, the control law

$$D^1 = \begin{cases} D_1 = \frac{K_{min}\mu_{1min}(S_1)}{S_{1in,max}-S_{1max}} & \text{if } S_1 > S_{1max} \\ D_2 = \frac{K_{max}\mu_{1max}(S_1)}{S_{1in,min}-S_{1min}} & \text{if } S_1 < S_{1min} \\ D_3 = \frac{D_1(S_1-S_{1min})+D_2(S_{1max}-S_1)}{S_{1max}-S_{1min}} & \text{if } S_{1min} \leq S_1 \leq S_{1max} \end{cases} \quad (40)$$

is strictly positive and it globally asymptotically stabilizes S_1 in (36) into the control pipe $[S_{1min}, S_{1max}]$.

Proof: It should first be pointed out that the control D^1 is continuous in S_1 .

a) Suppose that $S_1(0) > S_{1max}$, then $D^1 = D_1$ ensures that

$$\begin{aligned} \dot{S}_1 &= \frac{K_{min}\mu_{1min}(S_1)}{S_{1in,max}-S_{1max}}(S_{1in} - S_1) - K\mu_1(S_1) \\ &< \frac{K_{min}\mu_{1min}(S_1)}{S_{1in,max}-S_{1max}}(S_{1in}-S_{1max}) - K\mu_1(S_1) \\ &< K_{min}\mu_{1min}(S_1) - K\mu_1(S_1) \\ &< 0 \end{aligned}$$

which ensures convergence of S_1 towards S_{1max} .

b) Suppose that $S_1(0) < S_{1min}$, then $D^1 = D_2$ ensures that

$$\begin{aligned} \dot{S}_1 &= \frac{K_{max}\mu_{1max}(S_1)}{S_{1in,min}-S_{1min}}(S_{1in} - S_1) - K\mu_1(S_1) \\ &> \frac{K_{max}\mu_{1max}(S_1)}{S_{1in,min}-S_{1min}}(S_{1in}-S_{1min}) - K\mu_1(S_1) \\ &> K_{max}\mu_{1max}(S_1) - K\mu_1(S_1) \\ &> 0 \end{aligned}$$

which ensures convergence of S_1 towards S_{1min} .

c) Considering $D^1 = D_3$, we see that, in $S_1 = S_{1max}$, we have $\dot{S}_1 \leq 0$, and, in $S_1 = S_{1min}$, we have $\dot{S}_1 \geq 0$

From these three points, we conclude that the interval $[S_{1min}, S_{1max}]$ for S_1 is globally attractive and invariant. ■

Discussion: It could be very tedious to find all the equilibrium points of S_1 in (36) and to prove their stability when we close the loop with D^1 . In fact, besides the initial condition, the equilibrium points strongly depend on the uncertainties imposed by Assumption 10, which could change from a

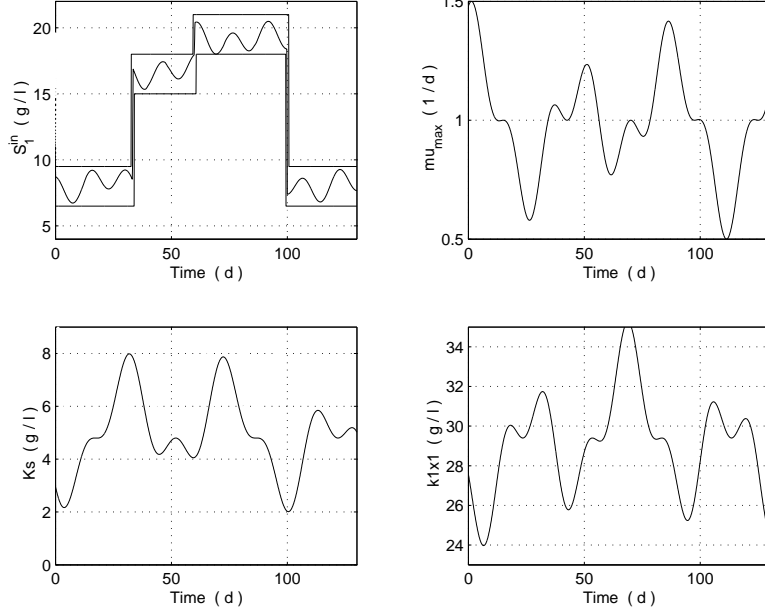


Figure 13: Parameter and input uncertainties

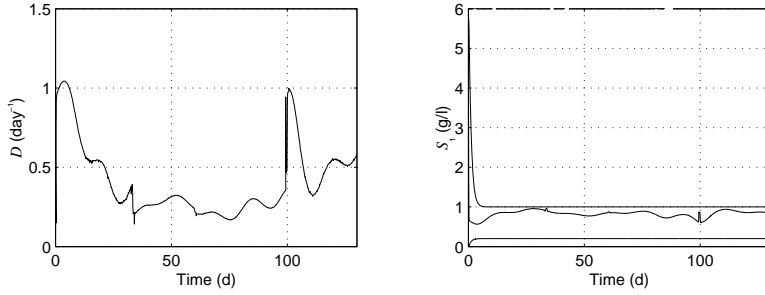


Figure 14: The regulation of S_1 and the regulation law, D

particular case to another. Notice, however, that we do not need to know neither these equilibrium points nor their stability properties. The important point is that the concept of stability suggested by (38) and (39) is sufficient to ensure that D_1 and D_2 will mandatory lead S_1 into the control pipe $[S_{1min}, S_{1max}]$. The equilibrium points all belong to the interval $[S_{1min}, S_{1max}]$.

The action of our controller is illustrated on Figure 14 in a case where $\mu_{1min}(S_1)$ and $\mu_{1max}(S_1)$ are functions that are defined from upper and lower bounds of the parameters that define the Monod Function $\mu_1(S_1)$ (K_{S_1} and μ_{1max}). The other parameters, K and S_{1in} , are also time-varying, and time-varying upper and lower bounds are illustrated on Figure 13.

2.4.2 The regulation of S_1 and S_2

Suppose that it is required to steer S_1 into an interval $[S_{1min}, S_{1max}]$ and S_2 into an interval $[S_{2min}, S_{2max}]$. We will present a method that approximately achieves this goal when the following

assumption is satisfied:

Assumption 11 *The intervals $[S_{1min}, S_{1max}]$ and $[\frac{k_1}{k_2}S_{2min}, \frac{k_1}{k_2}S_{2max}]$ overlap*

Let us now define

$$\begin{aligned} S_{Tmin} &= \max(S_{1min}, \frac{k_1}{k_2}S_{2min}) \\ S_{Tmax} &= \min(S_{1max}, \frac{k_1}{k_2}S_{2max}) \end{aligned}$$

The interval $[S_{Tmin}, S_{Tmax}]$ is then the interval upon which $[S_{1min}, S_{1max}]$ and $[\frac{k_1}{k_2}S_{2min}, \frac{k_1}{k_2}S_{2max}]$ overlap. We will then design a regulator that steers $S_T = S_1 + \frac{k_1}{k_2}S_2$ into this interval. By doing so, it will ensure that S_1 and $\frac{k_1}{k_2}S_2$ are smaller than S_{Tmax} , which means that S_1 is smaller than S_{1max} and S_2 is smaller than S_{2max} . However, ensuring the steering of S_T into an interval does not ensure that S_1 and S_2 satisfy their lower bounds. The controller that we propose does not achieve the specifications: instead of steering S_1 and S_2 into prespecified intervals, it steers S_T into an interval, while ensuring that S_1 and S_2 satisfy their prespecified upper bounds. The proposed controller is an extension of the controller that was presented in Section 2.2. It takes the form:

$$D^2 = \begin{cases} D_{T_1} = \frac{k_3 k_1}{k_2 k_4} \frac{q_{CH_4}}{S_{Tin,max} - S_{Tmax}} & \text{if } S_T > S_{Tmax} \\ D_{T_2} = \frac{k_3 k_1}{k_2 k_4} \frac{q_{CH_4}}{S_{Tin,min} - S_{Tmin}} & \text{if } S_T < S_{Tmin} \\ D_{T_3} = \frac{D_{T_1}(S_T - S_{Tmin}) + D_{T_2}(S_{Tmax} - S_T)}{(S_{Tmax} - S_{Tmin})} & \text{if } S_{Tmin} \leq S_T \leq S_{Tmax} \end{cases} \quad (41)$$

Following the lines of the proof of stability of the regulation of S_1 , it is easily proven that S_T is steered into an interval. The satisfaction of the upper-bounds for S_1 and S_2 is then a direct consequence of the choice of S_{Tmax} .

2.4.3 Conclusion

In this section, we have tentatively developed a controller that could simultaneously tackle the control of two different variables. This controller can take uncertainties into account, by considering upper and lower bounds on the parameters k_i or on the incoming substrate S_{Tin} . It is robust in achieving the regulation, because it does not force the substrate to converge towards a fixed value, but instead ensures the attractivity and invariance of an interval.

2.5 Conclusion

The control of the COD is the main control problem that has been tackled up to now. Four different controllers have been proposed. They all achieve the proposed control objective, when applied to the 2 or 4- dimensional models upon which they have been built. In addition, the static feedback of the methane flow rate of Section 2.2 has been shown to achieve good performance, when applied to a test bioreactor. Also, the adaptive feedback of the methane flow rate of Section 2.3 gives good performance when applied to the virtual plane based on the ADM1 model. The other two controllers still need to be tested in a realistic environment, but the methods that have been used for their construction make them robust controllers, so that we hope they will also give good performances when applied to a realistic plant (experimentally or virtually).

3 Control of the VFA concentration

A single approach has been developed for the control of this quantity; it has been developed in [27]. It is based on fuzzy logic, so that it does not rely on the development of a model of the anaerobic digester as much as the controllers that were presented in the previous sections. Similarly to the control of the COD, the control variable is the dilution rate. The treatment of VFA values through signal processing and fuzzy logic attempts to anticipate the behavior of the variable and to avoid the inherent delay of the response, associated to the time constant of the system.

As we have already hinted in the previous sections, the limiting step of the anaerobic digestion is often the conversion of the VFA into methane ([2]). Hence, VFA are intermediates which may accumulate provoking a decrease of reactor pH and the overall failure of the operation. The control of VFA concentration within the reactor, either directly or indirectly, is required in order to maintain the stability of the operation in variable-loaded reactors (this is the case of the majority of industrial plants). The most important drawback to fulfill VFA automatic control is the lack or the high cost of devices allowing its on-line measurement. To address this drawback some authors have developed and tested relatively inexpensive systems for the monitoring of, first, bicarbonate alkalinity ([15, 14]) and, later, VFA ([10]), using titration principles. The Laboratoire de Biotechnologie de l'Environnement of INRA at Narbonne developed such a sensor ([5]) capable to measure VFA, as well as partial and total alkalinity based on a titrimetric method, supplying one measurement every half hour (3 minutes if required) and having proven its reliability over a five year period of daily use.

The fuzzy-logic, that we use for the design of our controller was introduced by Zadeh in 1965, and constitutes an easy way to represent heuristic knowledge using linguistic labels implemented in linguistic rules. It presents the advantage of dealing with uncertainties and the non-requirement of complex mathematical relationships. The fuzzy inference process involves membership functions, fuzzy logic operators and knowledge rules. The membership functions allow the representation of a degree of membership to a fuzzy set, associated to a linguistic label, for a given input numerical value. The rules if-then introduce the expert knowledge in a computable way by means of the operators, which may be “and” & “or”. The fuzzy set theory has been discussed in detail by several authors ([34, 18]) and applied to anaerobic processes in some cases ([24, 12, 8, 11, 28, 25]).

3.1 Material and methods

3.1.1 Anaerobic wastewater treatment plant

Raw and diluted (1:2) industrial wine distillery effluents were anaerobically treated in a 0.948 m³ fixed bed upflow reactor. The results presented in this work correspond to operation with diluted wastewater (1:2) except those corresponding to the validation of the control law against a sudden increase in influent COD concentration. In those cases, diluted wastewater alternated with raw wastewater was fed to the system. The wastewater characterization is presented in Table 1. For this study, the interval between the titrimetric measurements was established at 30 minutes, as it was considered fast enough compared to the hydraulic residence time of the process (between 19 and 190 h) in order to obtain information about the operational state. The sensors are connected to an input/output device that allows the acquisition, treatment and storage of data on a PC using a modular software developed in our laboratory and freely available. This software is connected to

Component	Raw vinasses	Diluted vinasses (1:2)
Total COD (g/l)	26.40	13.20
Soluble COD (g/l)	23.60	11.80
VFA (g/l)	5.50	2.75
Total Suspended Solids	3.70	1.85
Volatile Suspended Solids	1.95	0.98
pH	5.20	5.20

Table 1: Typical characteristics of wine distillery wastewater

the MATLAB environment and allows the performance of different levels of advanced control and supervision. The modular software was used in this study as the platform for the implementation of the control law, object of study in this work. The interval of reception and sending of information between the software and the process was fixed at 2 minutes, as it was considered a good solution to be fast enough for control and supervision purposes, however generating reasonable size data files. The COD was measured off-line (NF T 90-101) following the principle of oxidation of the organic matter in excess of potassium dichromate and acid media (H₂SO₄) at boiling temperatures. The excess of dichromate is titrated by a solution of ammonium-iron sulfate.

3.1.2 Control Law

The fuzzy methodology applied was Mandani's fuzzy inference method ([23]). In this method, the first and the second part of the fuzzy inference process consist in the fuzzification of the inputs and application of fuzzy operators. Based on acquired knowledge on the process, a set of rules handling the regulation of the input flow rate in dependence on the concentration of VFA in the effluent of the reactor was set up. The controlled variable was the VFA concentration, with the manipulated variable being the input flow rate. We denote by ϵ the value of the VFA concentration minus the set point. In order to detect and identify in a clearer way the variation of VFA concentration, another variable, the derivative of VFA concentration, was generated ($\triangle \epsilon$). This second variable represents the velocity of change of VFA concentration and was used as input of the set of rules, together with the VFA concentration itself. The output of the control law was the degree of modification required for the influent flow rate in order to lead the system to achieve the desired set point ($\triangle F_{in} = \Delta D$). The first step to build the control law was the translation of possible values of the different inputs and output variables into linguistic labels given by membership functions. The summary of rules implemented in the control law is presented in Table 2.

In Figure 15, the membership functions for the inputs and output of the first approach to the control law are presented. An important aspect to carry out the distribution of membership functions is the consideration of the time interval to apply the control action. At this point, two intervals were considered: 2 and 30 minutes; given by the fixed interval of exchange of information between the software and the process and by the interval of analysis of the titrimetric sensor, respectively. The membership functions present some differences in terms of amplitude considering the possibilities: (i) reaction every 30 minutes having the actual concentration of VFA at this moment and (ii) reaction every two minutes having the actual concentration of VFA every 30 minutes. This last possibility (case ii) requires a more careful treatment of signal since the action of the controller

$\Delta\epsilon \setminus \epsilon$	gp	p	0	n	gn
n	gn	n	p	gp	gp
0	gn	n	0	p	gp
p	gn	gn	n	p	gp

Table 2: Summary of rules implemented in the control law. The first line represents the value of the VFA concentration minus the set point in g/l. The first column represents the value of the derivative of the VFA concentration in g/l min. The content of the table represents the increment or decrease of the actual input flow rate in l/h; gp : great positive; p : positive; 0 : no variation; n : negative; gn : great negative.

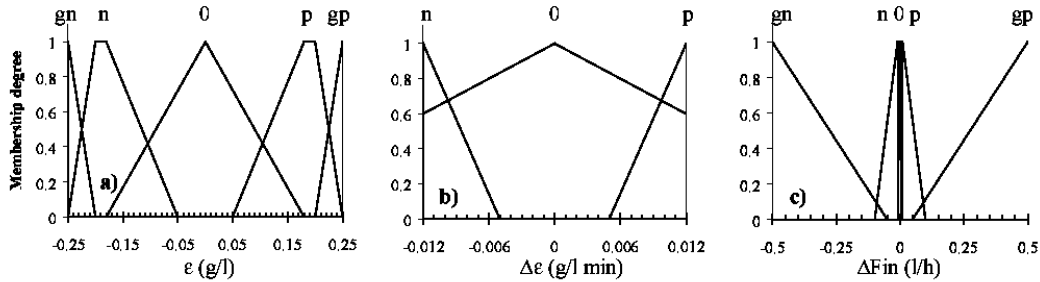


Figure 15: Membership functions of the input and output variables to the control law

is performed based on a value of VFA, which is not the actual value each two minutes. This was the reason to choose this approach. This approach was considered the most interesting one as it comprises the understanding of signal evolution to be implemented into the control law structure and could be used as well as basis for the other one. The extension to the case i) can be easily done by maintaining the distribution of membership functions for the actuation (ΔF_{in}) and increasing the interval from $[0.5, 0.5]$ to $[-10, 10]$ (data not shown). The relationship between the two inputs and the output of the control law is established by means of the set of rules. The surface of response according to the set of rules is presented in Figure 16. It is important to note that the intensity of response proposed for the region close to the set point is very small (showed in detail in Figure 16b) according to the established membership functions for ΔF_{in} (Figure 15c), due to the fast frequency of actuation (2 minutes). The non-linear variation of the response intensity for the different values of ϵ and $\Delta\epsilon$ represents the main advantage of this control law when compared to classical PID controllers based in the same process variables, while maintaining simple structure and implementation requirements.

3.2 Results and discussion

The first requirement for the proper performance of the control law was data treatment. For this purpose, a mean moving window applied to the last hour of data was used, as well as the removal of huge variations, due to signal displacement. Furthermore, in order to take into account the delay

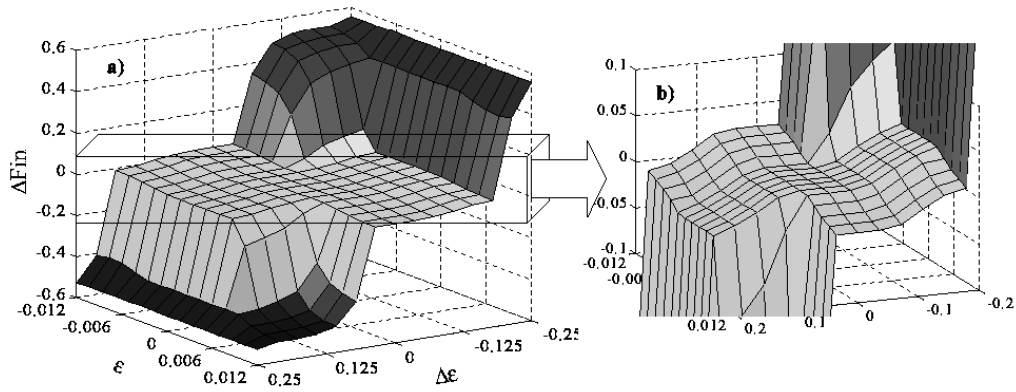


Figure 16: a) Surface of response of the law based on the divergence of VFA concentration from the desired set point (ϵ) and the variation of VFA concentration with time ($\Delta\epsilon$). b) Detail of the surface of response.

registered in the VFA concentration response to input flow rate variations, the prediction of VFA concentration evolution was also included in the law. The delay in the VFA concentration response is due to the time constant of the system and to the non registered response (one VFA value each 30 minutes) of the action (adjusted each 2 minutes) on the input flow rate. For this purpose, a simple algorithm predicting the next immediate values expected, according to the evolution (VFA derivative) during the last hour of process, was included.

The application was tested using both, data generated using a general model, which was developed and validated for the process ([4]), and real data from the process. The final on-line validation was performed in the fixed bed upflow reactor described above. The VFA concentration required at the output of the reactor, e.g. the set points of the control law, were set between 800 and 1800 mg/l. This range of concentrations, according to the performance previously observed in the process, was considered representative of the operation under different regimes, without attaining the destabilization of the reactor. An example of the performance of the control law is presented in Figure 17. The results presented correspond to 75 hours of operation, when switching the set point from 1000 to 1800 mg VFA/l. It can be observed that the control law led the process to a stable state in a short period of time (less than 10 hours), which represents the 19 % of the hydraulic residence time. However, some punctual disturbances must be pointed out. They are showed as insets in Figure 17 and they appear associated to noise from the VFA sensor. This induces some fluctuations of the response of the control law, which increases or decreases the input flow rate according to this fluctuations in VFA concentrations within the reactor. The sensitivity of this first approach of the control law to process disturbances, reflected in VFA concentration disturbances, represents an aspect to be improved, since the law responds to signal noise, which do not correspond to an event related to the process. In this sense, it was necessary to improve the signal processing procedure in order to distinguish between the different types of signal perturbation.

The modification of signal processing was performed by including an algorithm for linear/quadratic interpolation of VFA values in the moving window with respect to the previous one-hour measurements, and the corresponding extrapolation for the next half-hour. An example of results

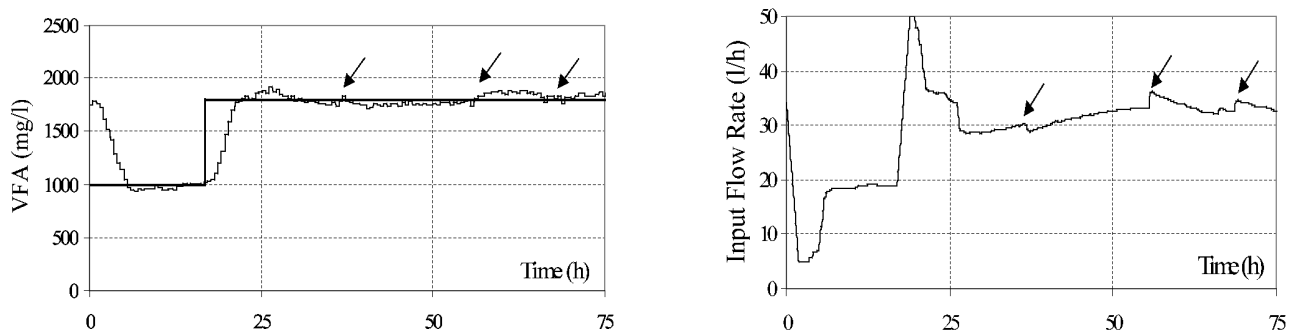


Figure 17: Results obtained from the on-line validation of the control law processing wine distillery wastewater of 10 g COD/l. The VFA concentration fixed as set point of the control law varied between 800 and 1800 mg/l (the thick line represents the VFA set-point and the thin line the VFA measure on the left figure). The insets correspond to signal disturbances, discussed in the text.

obtained with the control law following this procedure is shown in Figure 18. The set point for VFA during this interval of operation was changed from 800 to 1200 mg/l, back to 800 and the same change again up to 1200 mg/l, in order to observe the robustness of the control law. The starting point is a non-stable state, as the VFA are decreasing from a previous disturbance in the reactor. However, this event does not hinder obtaining a satisfying response from the control law, which adapt gradually the input flow rate from the minimum value of 5 l/h up to 12 l/h in 5 hours (less than 5 % of the HRT). The input flow rate established at this point by the control law remains stable until the next shift on the VFA set point (800 to 1200 mg/l on hour 27 of operation). The set point was maintained at 1200 mg VFA/l only from hour 27 to hour 32, because of an erroneous sensor measurement, marked with an arrow in Figure 18. This kind of defaults, corresponding to a lack of signal during a short period of time, pointed out to further modifications in signal processing. In fact, as the time constant of the system is much longer than the measurement interval, an extrapolation-estimation algorithm of VFA concentration can be done for at least one or two hours within an acceptable confidence interval. This procedure would avoid the shift in the response of the control action at hour 30, due to the failure of the VFA sensor and the lack of measurement during one half-hour. At that moment of operation, the input flow rate was fixed at 15 l/h during 2 hours, when the set point for VFA was fixed again at 800 mg/l and the control law was re-triggered. After hour 32 of operation, the good performance of the control law can be observed (Figure 18), attaining the desired VFA set point in 10 hours, which represent 10 % of the HRT in the reactor. Concerning the improvement in data treatment with extrapolation extended for 1-2 hours period, together with interpolation and elimination of high divergent measured values, an example of obtained results is showed in Figure 19. In this case, the extrapolation was done during two hours (arrow c), obtaining the agreement between the data supplied by the measurement device and previous extrapolated values after sensor restarting. Arrow a and b in Figure 19 point out two examples of correct elimination of highly divergent values provided by the measurement device. The effect of the interpolation procedure can be observed as well during the 40 hours monitoring interval presented in Figure 19, obtaining a quality signal, which contributes to the improvement of control law performance.

A typical disturbance in anaerobic digestors, together with variations in the input flow rate, is

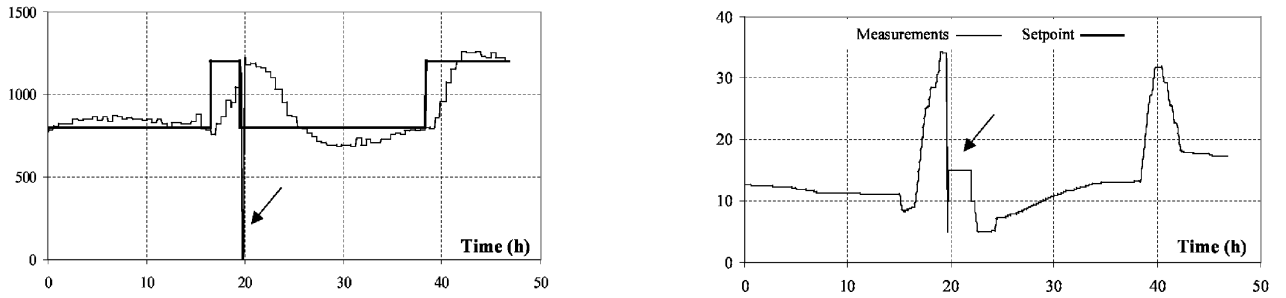


Figure 18: Results obtained from the on-line validation of the control law processing wine distillery wastewater of 10 g COD/l. The VFA concentration fixed as set point of the control law varied between 800 and 1200 mg/l (the thick line represents the VFA set-point and the thin line the VFA measure on the left figure). The insets correspond to signal disturbances, discussed in the text. The figure on the left represents the VFA and on the right, the input flow rate.

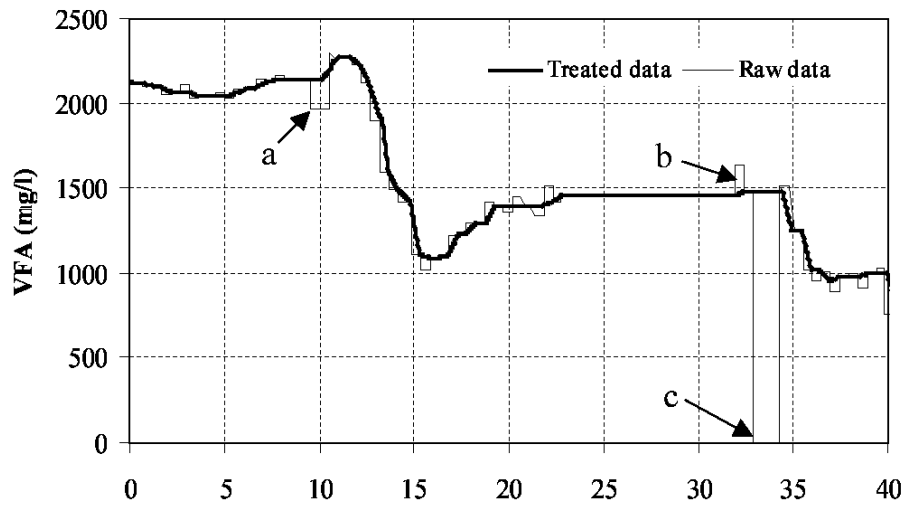


Figure 19: Comparison between raw values of VFA (measured each 30 minutes) and treated results after data treatment for the two minutes estimation (interval of actuation). The arrows point out the effect of elimination of high divergent values (a and b) and extrapolation (c) for estimation in case of absence of measured values during a one hour period.

the sudden change of influent COD, which usually is not detected in real time. The equalization tank previous to the reactor, present in many plants, makes a buffer effect on the influent COD to the reactor, which will change gradually as the complete volume of the tank is displaced. An aspect to point out is that, although the control law does not include the influent COD within the managed variables, it is adequate to test and validate it under influent COD changing conditions. This issue improved the performance of the control law and in general made it more suitable for real disturbances in real plants. The results of the on-line validation of the control law processing wine distillery wastewater with a gradual change of COD concentration are presented in Figure 20. For this purpose raw wastewater was suddenly fed to the system, obtaining a gradual increase in the COD (offline measured and presented in Figure 20a) directly fed to the reactor due to the effect of the equalization tank volume (0.2 m³). The influent COD achieves a stable value after approximately 5 hours of operation, the time needed to displace the volume of the equalization tank with the 50 l/h of influent flow rate at the starting point (Figure 20c). The VFA concentration fixed as set point of the control law was 1000 mg/l, which was maintained during the whole 50 hours in order to observe the performance of the controller until the stabilization of the system. The VFA within the reactor increased gradually (Figure 20b) together with the increase of the influent COD concentration, resulting in a decrease in the feeding flow rate estimated as output of the control law (Figure 20c). The feed flow rate stabilization was achieved approximately 20 hours after the perturbation, while less than 8 hours were needed to attain VFA values less than 20 % divergent from the desired set point. These results show the major difficulty to manage a changing COD concentration in the influent flow rate, when compared to changes in control (e.g. set points) purposes. However, the control law proposed can properly manage this sudden and usually not detected perturbation, leading the system to the appropriate operational conditions and maintaining a performing and stable behavior.

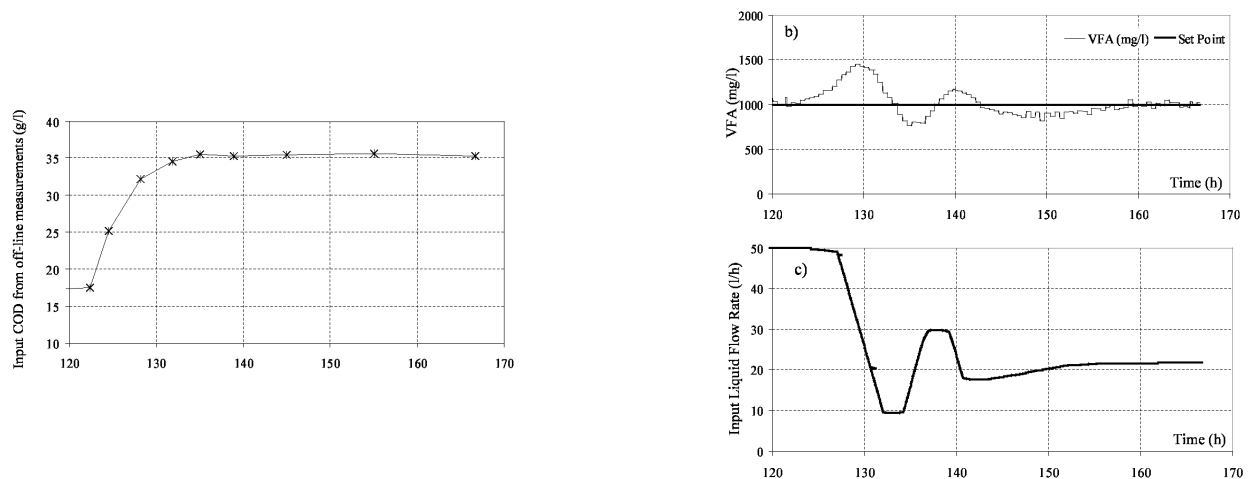


Figure 20: Results obtained from the on-line validation of the control law processing wine distillery wastewater with COD concentration changing gradually from 17 to 35 g COD/l (information not included in the control law). The VFA concentration fixed as set point of the control law was 1000 mg/l.

3.3 Conclusion

In this section, we have presented a control law based on fuzzy logic for the regulation of VFA concentration in the anaerobic digester. This was validated on a wastewater treatment process treating wine distillery wastewater. The validation was performed establishing different transient states between different set points in the range of 0.8 and 1.8 g VFA/l. This approach was tested as well for managing disturbances on COD influent concentrations (usually unknown by operators neither by the control law), which represent the usual situation, associated to the variations on process production in real plants. The sensitivity of the control law was optimized by interpolation, extrapolation and filtration procedures in order to avoid the undesired effect due to signal noise, without loosing sensitivity to detect disturbances of the process. The control law proved then to be reliable supplying an adequate control action in terms of amplitude and velocity to achieve the desired set point as well as to manage a sudden change in influent COD concentration. It is important to note that one of the main advantages of this approach is the simplicity in terms of used variables as well as for development and implementation, which may be comparable to a simple controller, but supplying a more satisfying performance.

4 Control of the cogeneration ratio

Another challenging problem in the control of an anaerobic plant is the regulation of the ratio $\frac{q_{CH_4}}{q_{CO_2}}$. This regulation problem is crucial if the methane that is produced by the plant is to be recycled as energy supply. We have not developed a controller that steers this quantity to the equilibrium yet, but we have performed a static analysis taking several parameters into account. Indeed, knowing that the dilution rate is used for the regulation of the COD or of the VFA concentration, we have little hope of having enough freedom with that control variable to also steer the cogeneration ratio. In this section, we investigate the effect of different parameters on the equilibrium value of the cogeneration ratio.

4.1 The model

We will be using an extension of model (1): the sixth-order model (AM1) that can be found in the Deliverable 3.1a. However, we will not stick to the formulation that was given in Deliverable D3.1a which contained the same states as (1) plus Z (the alkalinity) and C (the total inorganic carbon). Indeed, we are interested in evaluating q_{CH_4} (which we can easily obtain from S_2 and X_2) and q_{CO_2} , which we can obtain from a complicated chain of formulas that can be found in the Deliverable 3.1a. Upon observation of this chain, we see that C always appears within the expressions $C + S_2 - Z$. This quantity is an approximation of the CO_2 concentration. In fact, if we go back to the genesis of the model AM1, we see that the state C was built from S_2 , Z and the CO_2 concentration with the approximative formula $C \approx CO_2 - S_2 + Z$. Eliminating the C state and replacing it with a CO_2 state (that we will denote R in order to simplify the notations) gives a model that should be more accurate than the original AM1 model when considering quantities involving CO_2 (through the elimination of a step of approximation).

We then write

$$R = C + S_2 - Z \quad (42)$$

and the model is now:

$$\left\{ \begin{array}{l} \dot{X}_1 = (\mu_1(S_1) - \alpha D)X_1 \\ \dot{X}_2 = (\mu_2(S_2) - \alpha D)X_2 \\ \dot{Z} = D(Z - Z_{in}) \\ \dot{S}_1 = D(S_{1in} - S_1) - k_1\mu_1(S_1)X_1 \\ \dot{S}_2 = D(S_{2in} - S_2) + k_2\mu_1(S_1)X_1 - k_3\mu_2(S_2)X_2 \\ \dot{R} = D(R_{in} - R) + (k_4 + k_2)\mu_1(S_1)X_1 + (k_5 - k_3)\mu_2(S_2)X_2 - q_{CO_2} \end{array} \right. \quad (43)$$

The identification of the parameters of the (AM1) model has shown that $k_5 - k_3 > 0$. The expression of q_{CH_4} is the natural output of the system and is quite simple

$$q_{CH_4} = k_6\mu_2(S_2)X_2$$

The expression of q_{CO_2} is more complex:

$$q_{CO_2} = k_L a (R - K_H P_{CO_2})$$

where P_{CO_2} , the partial pressure of CO_2 , is the smallest root of the second order equation

$$K_H P_{CO_2}^2 - \phi P_{CO_2} + P_T R = 0 \quad (44)$$

the other root being larger than P_T ($\phi = K_H P_T + R + \frac{q_{CH_4}}{k_L a}$). This root is

$$P_{CO_2} = \frac{\phi - \sqrt{\phi^2 - 4K_H P_T R}}{2K_H} \quad (45)$$

From this, it is easily seen that system (43) is positive; indeed, if $R = 0$, we have $P_{CO_2} = 0$ from (45), which forces $q_{CO_2} = 0$, and $\dot{R} \geq 0$.

We want to regulate the ratio $\frac{q_{CH_4}}{q_{CO_2}}$; it is equivalent to regulate the ratio $\frac{P_{CO_2}}{P_T}$. Indeed, we have the natural relation:

$$P_{CO_2} = \frac{q_{CO_2}}{q_{CH_4} + q_{CO_2}} P_T$$

which leads to

$$\frac{q_{CH_4}}{q_{CO_2}} = \frac{P_T}{P_{CO_2}} - 1$$

Let us call $\alpha = \frac{P_{CO_2}}{P_T} \leq 1$, the proportion of the total pressure that comes from CO_2 . In the following section, the mathematical analysis will be made by studying this variable α , while the simulations represent the actual value of the ratio $\frac{q_{CH_4}}{q_{CO_2}}$. We will now study the dependence of the steady state of the cogeneration ratio on the variation of different system parameters.

4.2 Dependence of the equilibrium value with respect to D

The most natural variable that we could use for the control of the cogeneration ratio is the dilution rate D . Though this variable is already used for the control of the COD or the VFA concentrations, there might exist controllers which leave enough freedom for the use of the actuating variable to achieve other tasks.

As stated in the introduction of this section, we will perform a static analysis: for different values of constant dilution rate, we evaluate the value of the cogeneration ratio at the equilibrium. We perform several simulations on the model by fixing all the parameters at the identified values and $(S_{1in}, S_{2in}, R_{in})$ at some arbitrary values (Z_{in} does not play any role). We then impose the constant input D , and check the value of the ratio at the equilibrium. We then evaluate the value of the ratio at the equilibrium for several reasonable constant values of D , that is, values of D which do not cause a wash-out of the bacteria. Note that a wash-out of X_2 results in a methane gaseous flow rate that goes to zero, and a ratio $\frac{q_{CH_4}}{q_{CO_2}}$ that also goes to zero. This is illustrated on Figures 21 and 22; it can be seen that for $D > 1.08$, the cogeneration ratio goes to 0; this indicates that the bacteria X_2 have been washed out.

Several conclusions can be drawn from these pictures:

- the value of the ratio at the steady state is almost independent of the constant dilution rate, at least for reasonable values of D , which neither lead to a wash-out of the bacteria that generate the methane, nor to an important reduction of this population (e.g. limit D to the interval $[0, 0.8\bar{D}]$ where \bar{D} is the smallest value of D that leads to a wash-out). The dilution

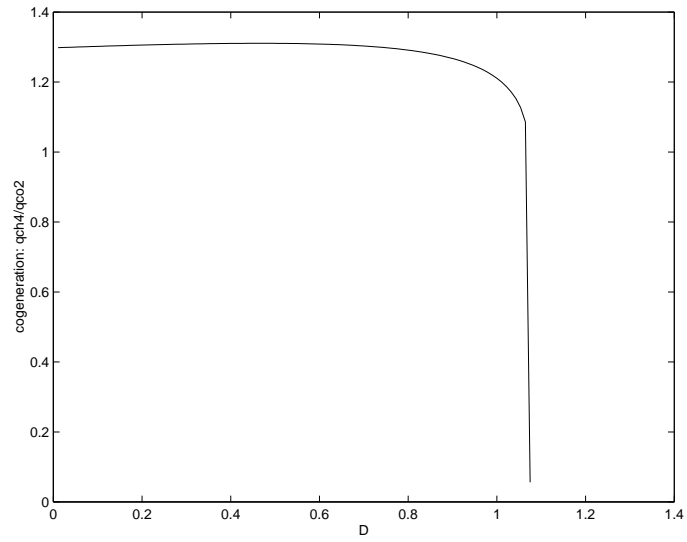


Figure 21: Evolution of the ratio at the equilibrium as a function of D . The free parameters have been fixed at $(S_{1in}, S_{2in}, R_{in}) = (40, 40, 20)$.

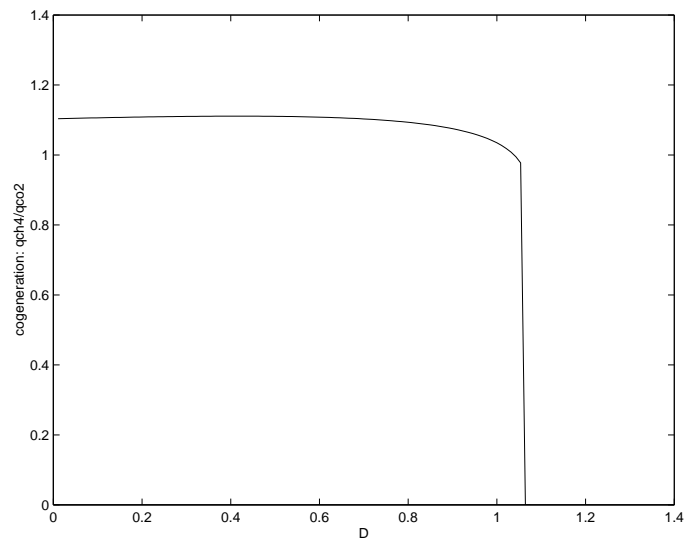


Figure 22: Evolution of the ratio at the equilibrium as a function of D . The free parameters have been fixed at $(S_{1in}, S_{2in}, R_{in}) = (60, 20, 2)$.

rate is therefore not a good control variable for the ratio. It could be used to prevent transient falls of the value of the ratio $\frac{q_{CH_4}}{q_{CO_2}}$, but it will almost be of no help to fix the value of the steady state.

- The attempt of regulating the ratio through D could even lead to critical behaviors: suppose that we are in the situation of Figure 22 with $D = 0.6$ and the ratio at about 1.1; suppose now that $(S_{1in}, S_{2in}, R_{in})$ switches to the value of Figure 21. An attempt of keeping the ratio close to 1.1 would necessitate D to take a value very close to \bar{D} , which is very undesirable.
- The value of the ratio is much more dependent on all the other parameters of the system (including $(S_{1in}, S_{2in}, R_{in})$). We will therefore pursue the analysis of the dependence of the steady state of $\frac{q_{CH_4}}{q_{CO_2}}$ on some other parameters.

4.3 Dependence of the equilibrium value with respect to P_T

A parameter upon which it is sometimes possible to act is the total pressure in the reactor (P_T). As we did in order to analyze the influence of the dilution rate on the steady state value of the cogeneration ratio, we now fix all the parameters except the total pressure, and plot the value of the steady state ratio on Figure 23. It is illustrated there that an increase of total pressure inside the plant results in an increase of the ratio $\frac{q_{CH_4}}{q_{CO_2}}$. The ratio linearly increases with the total pressure, but the slope is small. The ratio increases more or less by 0.05/atm. We have to wonder if it is useful to multiply the total pressure inside the plant by 10 (to go from 1 atm. to 10 atm.) to obtain an increase of 35% of the ratio $\frac{q_{CH_4}}{q_{CO_2}}$. Also, this increase of pressure must be feasible and the original model must stay valid despite this change of environment (also note that the pressure in a high industrial reactor is very different between the top and the bottom of the reactor). Following this remark, we do not investigate the influence of P_T any further.

4.4 Dependence of the equilibrium value with respect to $k_L a$

There are some parameters of the model that we can modify by a change of operating conditions; $k_L a$ is one of them. By increasing the recirculating flow in the plant, this parameter is increased. It is linked to the amount of CO_2 that can be exchanged between the liquid phase and the gaseous phase.

On Figure 24, we illustrate the equilibrium value of the cogeneration ratio as a function of the $k_L a$ parameter. We notice that $\frac{d\frac{q_{CH_4}}{q_{CO_2}}}{dk_L a} > 0$, so that it is interesting to have $k_L a$ as small as possible. However, this means that the amount of CO_2 that can escape the liquid phase is very small, which cannot be exactly realized in practice. There certainly exists a minimal value of $k_L a$ below which it is difficult to go. However, we see that the reduction of $k_L a$ can have a much more important effect on the equilibrium value of the cogeneration ratio than the modification of D or P_T , as was analyzed in the previous sections. We will now depart from simulations and more rigorously analyze the effect of $k_L a$ on the equilibrium value of $\frac{q_{CH_4}}{q_{CO_2}}$, through the analysis of α^* .

We start the analysis from equation (44), which is rewritten as:

$$K_H P_T \alpha^{*2} - \phi^* \alpha^* + R^* = 0$$

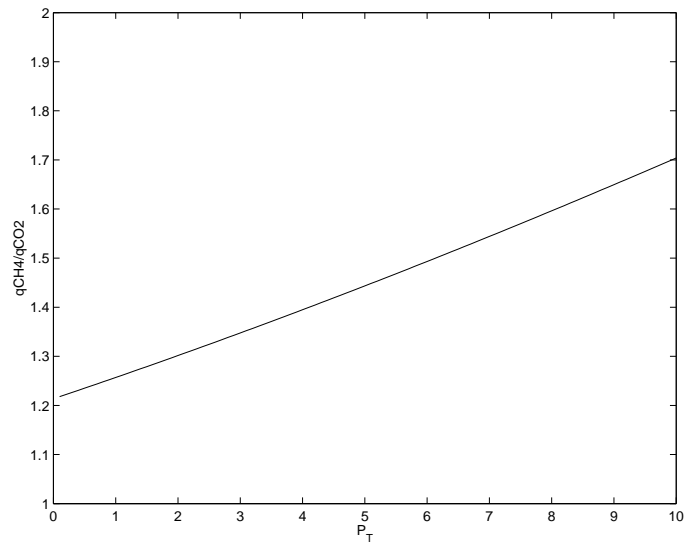


Figure 23: Evolution of the ratio at the equilibrium as a function of the total pressure in the plant. The free parameters have been fixed at $(S_{1in}, S_{2in}, R_{in}) = (40, 40, 20)$.

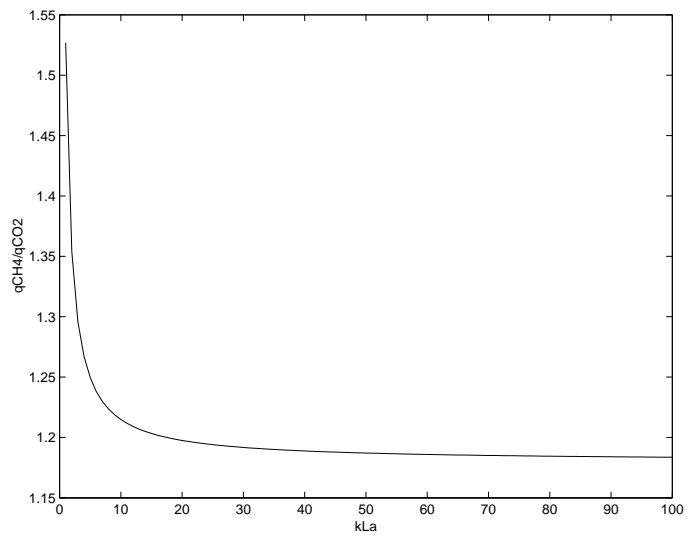


Figure 24: Evolution of the ratio at the equilibrium as a function of k_{La} . The free parameters have been fixed at $(S_{1in}, S_{2in}, R_{in}) = (40, 40, 20)$. The identified value of k_{La} is 19.6

Differentiating with respect to $k_L a$ results in

$$2K_H P_T \alpha^* \frac{d\alpha^*}{dk_L a} - \frac{d\phi^*}{dk_L a} \alpha^* - \phi^* \frac{d\alpha^*}{dk_L a} + \frac{dR^*}{dk_L a} = 0$$

From the expression $\phi^* = K_H P_T + R^* + \frac{q_{CH_4}}{k_L a}$, we see that

$$\frac{d\phi^*}{dk_L a} = \frac{dR^*}{dk_L a} - \frac{q_{CH_4}}{k_L a^2}$$

so that we have

$$2K_H P_T \alpha^* \frac{d\alpha^*}{dk_L a} + \frac{q_{CH_4}}{k_L a^2} \alpha^* - \phi^* \frac{d\alpha^*}{dk_L a} + (1 - \alpha^*) \frac{dR^*}{dk_L a} = 0$$

and

$$(2K_H P_T \alpha^* - \phi^*) \frac{d\alpha^*}{dk_L a} + \frac{q_{CH_4}}{k_L a^2} \alpha^* + (1 - \alpha^*) \frac{dR^*}{dk_L a} = 0$$

Remembering that $P_T \alpha^* = P_{CO_2}^*$ and equation (45), we see that

$$2K_H P_T \alpha^* - \phi^* = -\sqrt{\phi^{*2} - 4K_H P_T R^*}$$

so that, when $\alpha^* \approx 1$ (while staying smaller than 1 because of its definition), we have

$$-\sqrt{\phi^{*2} - 4K_H P_T R^*} \frac{d\alpha^*}{dk_L a} + \frac{q_{CH_4}}{k_L a^2} \alpha^* \approx 0$$

We then conclude that $\frac{d\alpha^*}{dk_L a} > 0$ when α^* is close to 1.

Translating this relation into the actual cogeneration ratio, it is easily seen that

$$\frac{d \frac{q_{CH_4}^*}{q_{CO_2}^*}}{dk_L a} < 0$$

when $\frac{q_{CH_4}^*}{q_{CO_2}^*}$ is small. This gives us a first way of improving the cogeneration ratio: if the cogeneration ratio is small, then we should reduce the $k_L a$ in order to increase the ratio.

4.5 Conclusion

In this part of this report, we have shown that very few parameters have a big influence on the steady-state of the cogeneration ratio. Notably, we have shown that the dilution D was a very bad control input for this task. The only studied parameter that has an important influence on the ratio is $k_L a$; we have evidenced this by simulations and by approximate analysis. We want to have $k_L a$ as small as possible to have a large cogeneration ratio. In the real plant, $k_L a$ can be increased by recirculating the output flow of the plant; this does not make sense if we want to have the cogeneration ratio as large as possible, but it can be a tool if the objective is to keep the cogeneration ratio constant despite change of operating conditions.

5 Conclusion

In this report, we have given control laws for the regulation of a model of anaerobic digestion with two bacteria. We first presented four control laws that could regulate the pollution level so that the legal pollution norm are satisfied at the output of the digester. Two of them ensures that the pollution level stays between a minimal and a maximal value. The other two achieve exact regulation at the desired set-point. We then presented a fuzzy controller that achieved VFA regulation; this regulation is often necessary to avoid acidification of the digester, which results in the death of the bacteria. We have then shown the influence of three parameters on the value of the ratio $\frac{q_{CH_4}}{q_{CO_2}}$, which is important to the cogeneration, that is the efficient methane production as a by-product of the anaerobic digestion. It is shown through simulations and approximate analysis that the most promising parameter that could influence the value of the cogeneration is $k_L a$ (and that D is especially ill-suited to that task).

References

- [1] G. Bastin and D. Dochain. *On-line Estimation and Adaptive Control of Bioreactors*. Elsevier, 1990.
- [2] D. J. Batstone, J. Keller, I. Angelidaki, S.V. Kalyuzhnyi, S.G. Pavlostathis, A. Rozzi, W.T.M. Sanders, H. Siegrist, and V.A. Vavilin. The iwa anerobic digestion model no.1 (adm1). *Water. Sci. Technol.*, 45 (10):65–73, 2002.
- [3] O. Bernard, Z. Hadj-Sadok, and D. Dochain. Advanced monitoring and control of anaerobic wastewater treatment plants : Dynamical model development and identification. In *Proceedings of Watermatex 2000*, pages 3.57–3.64. Gent, Belgium, 2000.
- [4] O. Bernard, Z. Hadj-Sadok, D. Dochain, A. Genovesi, and J. P. Steyer. Dynamical model development and parameter identification for an anaerobic wastewater treatment process. *Biotech. Bioeng.*, 75:424–438, 2001.
- [5] J.C. Bouvier, J.P. Steyer, and J.P.U. Delgenes. On-line titrimetric sensor for the control of vfa and/or alkalinity in anaerobic digestion processes treating industrial vinasses. In *Proceedings of the VII Latin American IWA Workshop and Symposium on Anaerobic Digestion (Merida, Mexico)*, 2002.
- [6] C. Chicone. *Ordinary Differential Equations with Applications*. Texts in Applied Mathematics. Springer, 1999.
- [7] D. Dochain and M. Perrier. Control design for nonlinear wastewater treatment processes. *Water Science and Technology*, 28:283–293, 1993.
- [8] M. Estaben, M. Polit, and J.P. Steyer. Fuzzy control for an anaerobic digester. *Cont. Eng. Pract*, 5 (98):1303–1310, 1997.
- [9] M. Farza, K. Busawon, and H. Hammouri. Simple nonlinear observers for on-line estimation of kynetic rates in bioreactors. *Automatica*, 34:301–318, 1998.

- [10] H. Feitkenhauer, J. von Sachs, and U.F.R. Meyer. On line titration of volatile fatty acids for the control of anaerobic digestion plants. *Wat. Res.*, 36 (1):212–218, 2002.
- [11] A. Genovesi, J. Harmand, and J.P. Steyer. A fuzzy logic based diagnosis system for the on-line supervision of an anaerobic digester pilot-plant. *Biochemical Engineering Journal*, 3:171–183, 1999.
- [12] E. Giraldo-Gomez and M.J.C. Duque. Automatic start-up of a high rate anaerobic reactor using a fuzzy logic control system. In *Proceedings of the V Latin American Workshop-Seminar on Wastewater Anaerobic Treatment (Vina del Mar, Chile)*, 1998.
- [13] G. W. Harrison. Global stability of predator-prey interactions. *Journal of Mathematical Biology*, 8:159–171, 1979.
- [14] F.R. Hawkes, A.J. Guwy, D.L. Hawkes, and A.G. Rozzi. On-line monitoring of anaerobic digestion: application of a device for continuous measurement of bicarbonate alkalinity. *Wat. Sci. Tech.*, 30 (12):1–10, 1994.
- [15] F.R. Hawkes, A.J. Guwy, A.G. Rozzi, and D.L. Hawkes. A new instrument for on-line measurement of bicarbonate alkalinity. *Wat. Res.*, 27 (1):167–170, 1993.
- [16] J. Hofbauer and K. Sigmund. *The Theory of Evolution and Dynamical Systems*. Cambridge University Press, 1988.
- [17] H.K. Khalil. *Nonlinear Systems*. Macmillan Publishing Company, 1992.
- [18] H.X. Li and V.C. Yen. *Fuzzy sets and fuzzy decision-making*. C.R.C. Press, Inc., Boca Raton, U.S.A, 1995.
- [19] L. Mailleret and O. Bernard. A simple robust controller to stabilise an anaerobic digestion process. In *8th International Conference on Computer Applications in Biotechnology, Modelling and Control of Biotechnological Processes*, pages 213–218, 2001.
- [20] L. Mailleret, O. Bernard, and J.P. Steyer. Robust regulation of anaerobic digestion processes. *Water Science and Technology*, 48-6:87–94, 2003.
- [21] L. Mailleret, O. Bernard, and J.P. Steyer. Nonlinear adaptive control for bioreactors with unknown kinetics. *Automatica*, 2004. in press.
- [22] L. Mailleret, J.-L. Gouzé, and O. Bernard. Nonlinear control for algae growth models in the chemostat. In *European Control Conference 03*, 2003.
- [23] E.H. Mandani and S.E. Assilian. An experiment in linguistic synthesis with a fuzzy logic controller. *International Journal of Man-Machine Studies*, 7 (1):1–13, 1975.
- [24] A. Muller, S. Marsili-Libelli, A. Aivasidis, T. Lloyd, S. Kroner, and C. Wandrey. Fuzzy control of disturbances in a wastewater treatment plant. *Wat. Res.*, 31 (12):3157–3167, 1997.
- [25] E. Murnleitner, T.M. Becker, and A. Delgado. State detection of overloads in the anaerobic wastewater treatment using fuzzy logic. *Wat. Res.*, 36:201–212, 2002.

- [26] M. Perrier and D. Dochain. Evaluation of control strategies for anaerobic digestion processes. *International Journal on Adaptive Control and Signal Processing*, 7:309–321, 1993.
- [27] A. Punal, L. Palazzotto, J.C. Bouvier, T. Conte, and J.P. Steyer. Automatic control of vfa in anaerobic digestion using a fuzzy logic based approach. In *Proceedings of the VII Latin American IWA Workshop and Symposium on Anaerobic Digestion (Merida, Mexico)*, 2002.
- [28] A. Punal, J. Rodriguez, A. Franco, E.F. Carrasco, E Roca, and J.M. Lema. Advanced monitoring and control of anaerobic wastewater treatment plants: Diagnosis and supervision by a fuzzy-based expert system. *Wat. Sci. Tech.*, 43 (7):191–198, 2000.
- [29] H.L. Smith and P. Waltman. *The theory of the chemostat: dynamics of microbial competition*. Cambridge University Press, 1995.
- [30] J.P. Steyer, J.C. Bouvier, T. Conte, P. Gras, and P. Sousbie. Evaluation of a four year experience with a fully instrumented anaerobic digestion process. *Wat. Sci. Tech.*, 45 (4-5):495–502, 2002.
- [31] J.P. Steyer, J.C. Bouvier, P. Gras, J. Harmand, and J.P. Delgenès. On-line measurements of cod, toc, vfa, total and partial alkalinity in anaerobic digestion processes using infra-red spectrometry. *Wat. Sci. Tech.*, 45 (10):133–138, 2002.
- [32] F. Viel, E. Busvelle, and J. P. Gauthier. Stability of polymerization reactors using I/O linearization and a high-gain observer. *Automatica*, 31:971–984, 1995.
- [33] U. Zaher, J. Rodriguez, A. Franco, P.A.O. Vanrolleghem, O. Bernard, Z. Hadj-Sadok, and D. Dochain. Application of the iwa adm1 model to simulate anaerobic digester dynamics using a concise set of practical measurements. In *Proceedings of the IWA Conference on Environmental Biotechnology (Kuala Lumpur, Malaysia)*, 2003.
- [34] H.J. Zimmermann. *Fuzzy sets theory and applicatins*. Kluwer-Nijhoff, Boston, USA, 1985.